Investigations Into the Immunomodulatory Mechanisms of Human Milk Extracellular Vesicles on CD4+ T Cells

Martin Vincelot
MSc student Infection and Immunity
Utrecht University
SOLIS-ID: 2888467
m.l.h.vincelot@students.uu.nl

Daily Supervisor: PhD candidate Alberta Giovanazzi
Examiner: Professor Marca Wauben
Second Reviewer: Assoc. professor Esther Nolte-t' Hoen

Division of Cell biology, Metabolism and Cancer
Department of Biomolecular Health Sciences
Faculty of Veterinary Medicine
Utrecht University

Table of contents

Lay Summary

Extracellular vesicles (EVs) are small lipidic spheric entities released by cells into all bodily fluids. Although their existence was only discovered recently, they are now known to play central roles in communication between cells of the body. In the lab, EVs from human breastmilk were recently shown to reduce the activation of major cells of the immune system: helper T cells. This could be a mechanism to avoid over-activation of the immune system in the infant's gut and thus promote healthy development and immunity. We are trying to figure out how EVs cause this.

In the human body, helper T cells are not always active. Generally, they are found flowing through the immune system in search of their antigen. The T cell Receptor is a protein at the surface of the T cells which recognizes this antigen. Upon recognition, a portion of the T cell receptor which extends within the cell kick-starts a chain of protein reactions within the cell. This 'cascade' of interactions ultimately contributes to cellular activation by interacting with genes. A similar process also occurs with another receptor called CD28 when it recognizes its target. Together, the stimulations of TCR and CD28 lead to T cell activation.

We noticed that the inhibition of helper T cell activation by milk EVs was fast. Therefore, we suspected the milk EVs to directly interfere with the activation cascades instead of manipulating T cell genes for example. The milk EV cargo is diverse and contains many biomolecules which could be responsible for this effect. Thankfully, previous work done within the lab showed that milk EV cargo proteins could potentially interact with cascades of T cell activation. Therefore, we decided to study the proteins of milk EVs closely and to generate a list of candidates which we think contribute to T cell inhibition. Also, because it is difficult to study this mehanism within T cells from human blood, we decided to use a representative model: Jurkat cells. These are cancerous cells which keep some common characteristics with healthy T cells but are easier to manipulate for research purposes. Additionally, these Jurkat cells used were previously genetically modified to emit three differently colored fluorescent signals representing the activity of three main T cell activation cascades. We adapted this system to measure the EV effects on these three cascades of T cell activation.

The system was able to perfectly measure EV-caused reductions in the cell cascades and therefore activation. Interestingly, EVs from allergic donors were much less capable of reducing activation than those of healthy donors.

Overall, this research project led to the optimization of a system to study immune signaling cascades in T cells. Also, it heavily contributed to the understanding of how breastmilk interacts with the immune system of the infant, and the impact of allergy on this process. This holds great importance from a public health perspective as it could lead to updated medical advice around breastfeeding or baby formula compositions and ensure that infants develop healthy gut tissue and immunity.

Abstract

Human breast milk plays a major role in the development of the mucosal adaptive immune system of the newborn: passive immunity is transferred, antigens are shared to train lymphocytes, and recently – milk Extracellular vesicles (EVs) were shown to increase the threshold of activation of CD4+ T helper cells. EVs are nanosized lipid bilayered vesicles present in all bodily fluids and known to mediate intercellular communication via their surface and cargo. We believe that these inhibitory milk EVs hold a central role in maintaining immune peripheral tolerance in the infant's gut mucosa, thus allowing proper training and development of the tissues. However, the exact mechanisms by which EVs modulate T cell activation are unknown. The transient and reversible dynamics of this inhibition suggest that the EV contains a 'ready to act' cargo which could interfere with signaling pathways of T cell activation. In parallel, recent proteomic analysis was performed which unraveled a multitude of milk EV cargo proteins capable of interfering with pathways of T cell activation. To further investigate the potentially immunomodulatory nature of the milk EV protein cargo, an in-silico analysis of the proteomic results was performed hand-in-hand with the optimization of a Jurkat reporter cell line to better measure and compare EV-mediated immunomodulation of three canonical pathways of T cell activation. Once optimized, this system confirmed that milk EVs target TCR- and CD28- derived pathways to cause this inhibition. It also revealed that milk EVs from allergic parents are not able to inhibit CD4+ T cell activation as well as milk EVs from on-allergic donors. Overall, these fundamental insights

Introduction

In the first two years of its life, the newborn undergoes training of its adaptive immune system. Although the infant immunity encounters antigens in-utero, the birth of the infant is characterized by a sharp increase in antigen exposure and therefore the beginning of the adaptive system's training. The goal of this training is to learn to effectively differentiate between harmful and tolerated antigens (Semmes, E. C., et al., 2021).

T cells hold a central role in adaptive immunity: Humans with deficiencies in T cell functions often present weak immunity and higher vulnerability to infections. CD4+ helper T cells strongly influence the immune response: Depending on the cytokine environment, an activated CD4+ T cell can adopt a pro-inflammatory phenotype like Th1 just as it can differentiate into a regulatory T cell which halts immune responses. Once activated, pro-inflammatory CD4+ T cells heavily contribute to kick-start various arms of immunity. For instance, they can contribute to B cell activation and their differentiation into antibody-producing plasma cells. They can also produce pro-inflammatory cytokines which stimulate various cells of innate immunity.

As a result of this important immunostimulating potential, CD4+ T cell activation is tightly regulated. Its activation requires three main signals. As a first signal, CD4+ T cells are canonically activated via T cell receptor (TCR) recognition of its specific epitope presented on a Major Histocompatibility Complex II (MHC II) molecule. This antigen-derived epitope is presented after phagocytosis and processing by professional Antigen Presenting Cells (pAPCs). By binding to pAPC-specific MHC II -and not MHCI- molecules, the CD4 co-receptor ensures that the helper T cell activation occurs in the context of antigen presentation. Upon TCR binding, intracellular Immunoreceptor Tyrosine based Activation Motifs (ITAMs) of the TCR-associated CD3 molecule are phosphorylated by LCK, leading to the binding of ZAP-70 (Meuer, S. C., Fitzgerald, K. A, 1983, van Leeuwen, J. E., 1999, Chan, A. C., et al., 1992). This allows the initiation of several intracellular signaling cascades including the p38-MAPK pathway and the Calcium pathway which ultimately lead to "Activator protein 1" (AP-1) complex and "Nuclear factor of Activated T cells" (NFAT) translocation to the nucleus, respectively. Once both transcription factors (TFs)

are in the nucleus, NFAT and AP-1 form a complex which increases the expression of genes of T cell activation (cf. Fig.1).

CD28 is a well-established co-stimulatory receptor present on T cells which amplifies the TCR-resulting signal. Upon binding to its ligand, CD28 stimulates the PI3K-Akt pathway which ultimately leads to the transcription factor "Nuclear factor kappa-light-chain-enhancer of activated B cells" (NF-kB) translocation to the nucleus (cf. Fig.1). This importance of CD28 stimulation s highlighted by the anergy and retention of a naïve T cell phenotype which follows CD28 inhibition (Harding et al., 1992).

CD4+ T cells are found circulating in the lymphatic system where they can encounter pAPCs in secondary or tertiary lymphoid tissues. Mucosa-associated Lymphoid Tissues (MALTs) are clusters of adaptive immune cells located right under the mucosal epithelial linings. In MALTs, these CD4+ helper T cells sample the mucosal antigens processed and presented by pAPCs (Turner,

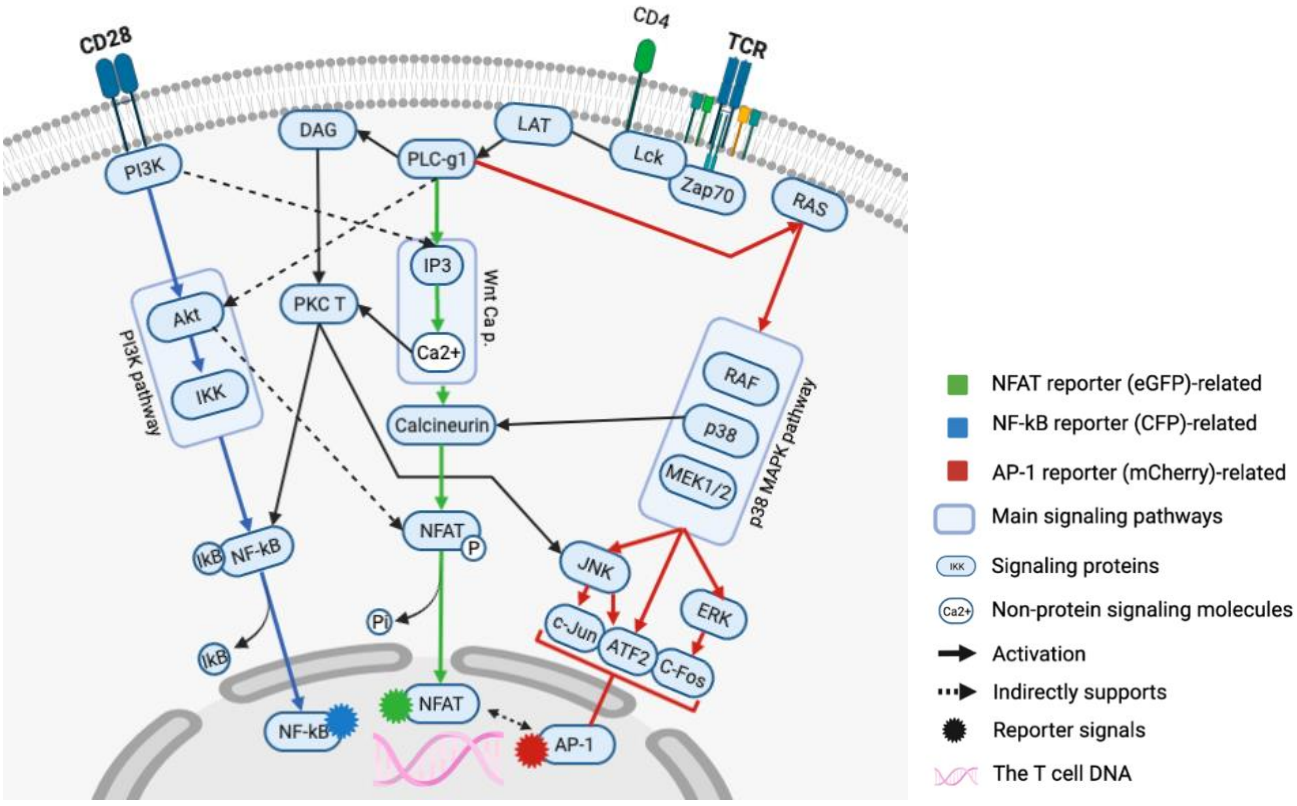

Fig. 1: Scheme of the main pathways of T cell activation: Stimulation of the T Cell Receptor/CD3 complex engages the Calcium and p38-MAPK pathways which ultimately result in NFAT and AP-1 translocation to the nucleus (signal 1). Moreover, CD28 stimulation is known to stimulate the PI3K-Akt pathway, resulting in NF-kB translocation to the nucleus (signal 2). Various direct and indirect cross-overs between the signaling pathways are also represented here. Made via Biorender.

D. L., & Farber, D. L., 2014). In the case of a newborn, oral and gut mucosal surfaces are overwhelmingly exposed to new antigens such as food and commensal bacteria. Without proper regulation of these T cells, Over-active or immature mucosal immunity is known to cause inflammation and prevent healthy microbiota formation (Mowat, A. M. et al., 2018). Pathologies known to emerge from such causes include necrotic enterocolitis (NEC) (Claud, E. C., (2001), autoimmunity and allergy. CD4+ T cell tolerance to commensal and food antigens is thus crucial in maintaining a balanced immunity at mucosal surfaces (Mowat, A. M. (2018). Interestingly, human breastfeeding was proven to reduce the likelihood of developing NEC and allergies. (Gopalakrishna, K. P., et al., 2019, Gdalevich, M., et al, 2001).

Human milk is a complex fluid mainly composed of milk fat globules, casein micelles, whey (soluble proteins), cells and antibodies (Pereira et al., 2014; Andreas, N. J., Kampmann, 2015). Among other functions, human milk inhibits the newborn's mucosal immunity (Catherine J Field et al., 2005) and provides passive immunity via parental antibody transfer (Palmeira, P., Quinello) . Human milk also includes extracellular vesicles (EVs). These are nanosized, lipid bilayer-enclosed vesicles which are selectively packaged with nucleic acids, lipids, and proteins for intercellular communication (Yáñez-Mó M et al.). They are heterogeneous in size and composition and can be derived from endosomal compartments (exosomes) or bud from the cellular membrane (microvesicles among others) of various cell types (Tkach, M., Kowal, J., et al., 2018). They can interact with target cells through membrane-membrane interactions (Zitvogel, L., et al., 1998) and can modulate the target cell via delivery of their cargo to the cytosol or endosomal compartments (Varcianna, A., et al., 2019). EVs were found in all human bodily fluids, including human milk (Lässer C et al.). Milk EVs are themselves incredibly diverse and were shown to present time-dependent and inter-donor variation in composition. Among other effects, milk EVs were proven to significantly inhibit CD4 + T cell activation in-vitro (Zonneveld et al., 2021). While EVs harbor a wide range of immunomodulatory micro RNAs (miRNAs) in their cargo (Zhou Q, et al., 2012), the instantaneous and transient characteristics of the observed inhibition discarded the hypothesis that genetic manipulation was responsible. On the contrary, it suggested that milk EVs possess a ready-to-act cargo of mediators which either directly affect receptor signaling or their resulting pathways of T cell activation (Zonneveld et al., 2021). A study on human milk EV proteins identified a unique proteome in milk EVs compared to other components of the milk (Martijn van

Herwijnen et al., 2016). These results strongly suggest that EV cargo proteins play an important role in milk EV-mediated T cell modulation. A follow-up enrichment analysis for major cellular processes was performed on the milk EV proteome. A list of potentially immunomodulatory milk EV proteins was compiled by selecting Gene Ontology (GO) terms related to T cell activation (Zonneveld et al., 2021). Mainly, the milk EV proteome was found to overwhelmingly harbor interactions with components of the co-stimulatory CD28-derived pathways.

The overarching goal of this research project is thus to investigate a causal link between the milk EV proteome and signaling pathways involved in T cell activation, with a particular focus on CD28 derived pathways.

To reach this goal, a list of milk EV cargo proteins which might regulate T cell activation signaling pathways was generated from the proteomic study previously mentioned. Because signaling pathways are heavily regulated through phosphorylation, kinases (enzymes catalyzing the addition of a phosphate group on their target protein) and phosphatases (enzymes catalyzing the hydrolysis of a phosphate group on their target protein) present in all samples used in the milk EV proteomics analysis underwent a systematic in-silico analysis to identify potential direct regulators.

To study the observed milk EV-mediated immunomodulation, a robust and effective read-out system for the activation or inhibition of the main T cell signaling pathways was needed. Interestingly, such a system was previously established using a Triple Parameter Reporter (TPR) E6.1 Jurkat cell line. E6.1 Jurkat cells are immortalized lymphoblasts which have commonly been used as models for T cell signaling research (Abraham, R. T., & Weiss, A. 2004). This system was originally established to test the activation potential of transgenic autologous T cell receptors (TCRs) designed in the context of Chimeric Antigen Receptor (CAR-T) cell therapy research. Importantly, the TPR cell line used in this project was not engineered in respect to TCR expression and was confirmed to express endogenous TCR only. However, this Jurkat cell line was engineered to express fluorescent reporters representing the levels of activity of three major downstream transcription factors of T cell activation: NFAT, NF-kB and AP-1. The genetic constructs used to engineer the cells are composed of a response element (RE) for each transcription factor, a minimal promoter, and the gene for the corresponding fluorophore (Jutz, S., et l., 2016). Therefore, reporter fluorescence intensity is directly correlated to the activity level of its corresponding transcription

factor. This system thus reports the activation status of the pathways leading to TF translocation into the nucleus. The main pathways involved in NF-kB, NFAT and AP-1 translocations were also hypothesized as targets of the milk EV proteome: the TCR- and most importantly CD28- derived pathways (cf. Fig 1). For NF-k However, to use this system to investigate EV-mediated CD28 (and other) pathway modulations, the activating condition had to be optimized: First, it needed to be strong enough to allow measurement of inhibition. Secondly, this same activation condition had to feed into CD28-derived pathways as much as possible. Following optimization of TPR activation, different EV samples were used to validate the system, and further in-silico work was performed to interpret the EV-mediated immunomodulation patterns.

Materials and Methods

I - In silico analysis of EV cargo kinases/phosphatases

First, a literature search regarding canonical TCR/CD3 and CD28-mediated pathways of T cell activation was performed. For this, the REACTOME database (Gillespie, M., et al., 2022) was used in combination with an extensive literature search on pathways of T cell activation. A summary scheme featuring the main actors of the pathways of T cell activation was produced via Biorender.com.

Then, a list of EV cargo kinases and phosphatases was retrieved from the previously generated proteomics study (van Herwijnen, MJC., et al, [mcp.M116.060426-1, “milk-derived EV”]). The list was processed through the Uniprot and the Human protein Atlas databases, as well as the enrichment analysis performed previously (Zonneveld et al (2021) [Supplementary file 3 (s3), “Interactions in pathways”]) for potential interactions with pathways of T cell activation. Furthermore, a literature search was performed on all candidates with the following key words: “[kinase name]” + “T cell activation”/ “signaling for furter information.

To determine whether the identified targets of these kinases/phosphatases were expressed in activated CD4+ T cells, they were processed through the DICE database (Schmiedel, B. J., et al., 2018).

The candidates that were shown to interact (activation or inhibition) with pathways of interest and which had their target highly expressed in activated CD4+ T cells were selected as main candidates. They were also added to the T cell activation scheme, where a color code was set up to differentiate T cell pathway components and EV cargo kinases or phosphatases.

II - Milk sample collection.

The milk samples from allergic and non-allergic donors were collected in the context of the ACCESS study (NL 47426.099.14; RTPO 914) which was approved by the local Medical Ethics Committee (Martini Hospital, Groningen, The Netherlands). All donors who took part of this study signed an informed consent form. Donors were defined as allergic when their total serum Immunoglobulin E (IgE) counts were equal or higher to 50 kU/mL and/or if specific IgE were detected for grass pollen, tree pollen, house dust mite, cat dander, or dog dander by positive Phadiotop assay results (Thermo-Scientific). More information in Supplementary document **Fig**. S4.

The milk samples from which EVs were isolated for all other experiments were collected from their donors (D40, D60, D54) less than fifteen months post-partum. Fore and hind milk from one breast was collected using an electric pump by the donors themselves, and then gently mixed before aliquoting 10-50 mL in sterile containers. The samples were transported to the lab in warm conditions and processed within 20 minutes. All donors provided their informed consent to participate in this study, which was approved by the local ethics committee

III- EV Isolation procedure

All milk samples were collected previously: the samples from allergic and non-allergic donors were collected in the context of the ACCESS study. To remove cells and the cream layer, all samples were previously centrifuged at 3000g for 10 minutes, at 22 degrees Celsius (Beckman Coulter Allegra X-12R, Fullerton, CA, USA). After removal of the top fatty layer using a spatula, the supernatants were transferred to new tubes and the centrifugation and fat removal steps were repeated. All samples were then biobanked at -80 degrees Celsius.

When needed, the supernatants were thawed at room temperature until a small clump of ice remained, and transferred to polyallomer 12.5 mL open SW40 ultra-centrifuge tubes (Beckman Coulter, ref: 331374). The milk supernatants were then centrifuged at 5000g for 30 minutes, at 4 degrees Celsius to remove large debris and residual cream (Beckman Coulter Optima XPN-80, SW40Ti rotor).

After removal of the fat layer, a 10 000g ultra-centrifugation step was performed at 4 degrees Celsius for 30 minutes (Beckman Coulter Optima XPN-80, SW40Ti rotor) to remove smaller cellular debris.

Then, 6.5 mL of the supernatants were transferred drop-by-drop onto carefully deposited 15-layered iodixanol gradients (from 60% to 10% from bottom to top) in SW40 tubes (OptiprepTM 60% Axis Shield, Cat: 1114542). The differently concentrated Iodixanol layers were made using 1x Phosphate Buffered Saline (PBS) at a pH of 7.2 (Gibco, Ref: 20012-019) as described in **Fig**. S5. Gradient ultracentrifugation at 192 000g (Beckman Coulter Optima XPN-80, SW40Ti) for 15 to 18 hours at 4 degrees Celsius then followed. The 6.5 mL supernatant was processed through an identical gradient ultra-centrifugation step to obtain a donor-specific procedural control: the EV-depleted sample. The gradients of both EV and EV depleted samples were then fractioned in volumes of 500uL. The optical densities of these fractions were all measured using a refractometer. Densities between 1.06g/ml (Refractive Index (RI) = 1.351) and 1.19g/ml (RI =1.392) were pooled. In previous work, these densities were determined to yield highest amounts of EV surface marker CD9 in western blot analyses (data not shown).

Both EV and EV depleted samples were run through 20mL Size Exclusion Chromatography (SEC) columns (Econo-Pac Disposable Chromatography columns Bio-Rad Laboratories, Hercules, CA, USA) packed with 17-20 mL of Sephadex *g*100 (Sigma-Aldrich, G100120-100G) to exchange iodixanol with 1x phenol-free Roswell Park Memorial institute (RPMI) 1640 medium (Gibco, ref: 11835-063). From the moment the samples were added to the column, the third to ninth millimeters of flow-through were collected. This knowledge is based on previous lab analysis which identified this volume as containing the highest protein concentrations and the highest detection of EV-associated marker CD63 (data not shown). These samples were then stored at -80 degrees Celsius. Later, the samples were thawed at room temperature and aliquoted in 500uL fractions before being refrozen at -80 degrees Celsius.

The concentrations of EVs in the stocks are comparable to physiological conditions, as the eluate volume collected of 7 mL (which was shown to contain almost all the EVs) was similar to the 6.5 mL of sample used for gradient ultracentrifugation. This EV isolation procedure was performed in semi sterile conditions: samples were always handled in a laminar flow hood, except during the SEC step.

IV - TPR Jurkat cell line

To generate the TPR system, E6.1 Jurkat cells were previously engineered to express three fluorescent reporters directly regulated by transcription factors downstream of canonical pathways of T cell activation. The three constitutional reporters are Green Fluorescent Protein (eGFP) for NFAT levels, Cyan fluorescent protein (CFP) for NF-kB levels, and mCherry for AP-1 levels (Rosskopf S., et al., 2018). Previous analysis of cell surface CD3 and CD28 levels showed comparable CD28 but reduced CD3 expression on the TPR Jurkat cell line compared to non-engineered Jurkat cells (data not shown).

V - TPR Jurkat cell culturing

TPR cells were previously stored in 1mL vials in liquid nitrogen. The cells were thawed until a small clump of ice was left, and then immediately diluted in 1 mL of culture medium: 1x RPMI 1640 with GlutaMax (Gibco, ref: 61870-010) enriched with 10% Fetal Bovine Serum (FBS) (Bodinco BV, BDC15642) and 1% penicillin/streptomycin (p/s) (Gibco, 15140-122). After incubation within a T25 flask with a filter screw (Cellstar, Rev: 02F010810) and cellular proliferation, the culture volume was increased to 10mL. From then on, cells were always passed twice a week at concentrations ranging from 40 000 to 100 000 cells/mL in RPMI, with a total of 10mL. The cells were cultured in T75 flasks with a filter screw (Cellstar, Rev: 02F010013) and incubated at 37 degrees Celsius, 5% Carbon dioxide (CO2) and humid conditions.

VI - TPR Jurkat activation experiments

In all experiments performed using the TPR Jurkat read-out system, phenol-free RPMI enriched with 1% p/s (Gibco, 15140-122) and 10% FBS (Bodinco BV, BDC15642) used. The same medium was further enriched with 1% Ultra glutamine (Lonza, BE17605E/U1) for the experiments involving extracellular vesicles. In all cases, culture-treated flat-bottom 96 well plates (Corning Costar, Ref: 3599) were used to incubate the TPR cells in different conditions. Unstimulated cells

were always used as negative control. Except for EV samples, the conditions were systematically set up in triplicate. The EVs were stored in phenol-free RPMI without additives, so 10% of FBS, 1% of p/s and 1% of ultra-glutamine were always added after thawing to match the experimental medium. In each well, 150 uL of EV/EV depleted samples were placed first. Then, 25uL of cells at 4 million cells/mL were added to reach a final amount of 100 000 cells in well. Finally, 25uL of stimulus was added, reaching a final volume of 200 uL. The plates were then incubated at 37 degrees Celsius, 5% Carbon dioxide (CO2) and humid conditions for varying periods of time depending on the experiment. After incubation, reporter signals were measured at the Flow cytometer (cf. **Fig**. 2). The plates were always handled in the lateral flow hood or kept with a lid to ensure sterile conditions. In the case of Phorbol 12-myristate 13-acetate (PMA) stimulation (Sigma-Aldrich, Ref: P1585 1mg/mL in DMSO), the original stock was previously diluted to reach 50 ug/mL in RPMI and then aliquoted and stored at -20 degrees Celsius. For Ionomycin (Sigma-

Fig.2: Scheme summarizing the rationale of the Triple Parameter Reporter (TPR) activation experiments. Upon stimulation, reporter signals representing the activation levels of three transcription factors of Jurkat cell activation are measured: NFAT-(eGFP), NF-kB-(CFP), mCherry-(AP-1). Made via Biorender.com.

Aldrich, Ref: 10634, 1mg/mL in phenol free RPMI), its original stock was previously aliquoted and stored at -20 degrees Celsius. regarding anti-CD3 (Sanquin, ref: M1654) and anti-CD28 (Sanquin, ref: M1650), the stocks were. Concanavalin A powder (Sigma-Aldrich, ref: 097K7670) was dissolved in phenol free RPMI at 1mg/mL, aliquoted and stored at -20 degrees Celsius.

VII - Flow cytometry

After incubation, cells were placed on ice to interrupt all biochemical reactions. Cell were re-suspended and centrifuged for 3 minutes at 1200 revolutions per minute (rpm) and 4 degrees Celsius. After discarding or storing their supernatants, the cells were re-suspended with 100uL of Fluorescence-Activated Cell Sorting (FACS) buffer [5% FBS in 1x PBS]. An identical centrifugation step then followed before discarding the supernatant and re-suspending the cells in 150uL of FACS buffer. Reporter fluorescences were measured on a CytoFLEX LX flow cytometer (Beckman Coulter. Serial number: BA12013). No staining were required for this cell line as the intracellular reporters are fluorescent. The eGFP reporter was stimulated using a 488 nm laser and its emission spectrum was captured with the 520-545 nm optical filter. For CFP, the 405 nm laser and the 520-545 nm optical filter were used. Finally, mCherry was measured using the 561 nm laser and the 610-620 nm filter. The acquisition gains were kept constant for all experiments (cf. **Fig** S6) No compensation was required as the laser beams are co-linear. Results were analyzed using FlowJo (version 10.1). The gating strategy reproduced in all experiments involved selecting the live cell population observed on Forward Scatter (FSC-A) versus Side Scatter (SSC-A) plots,

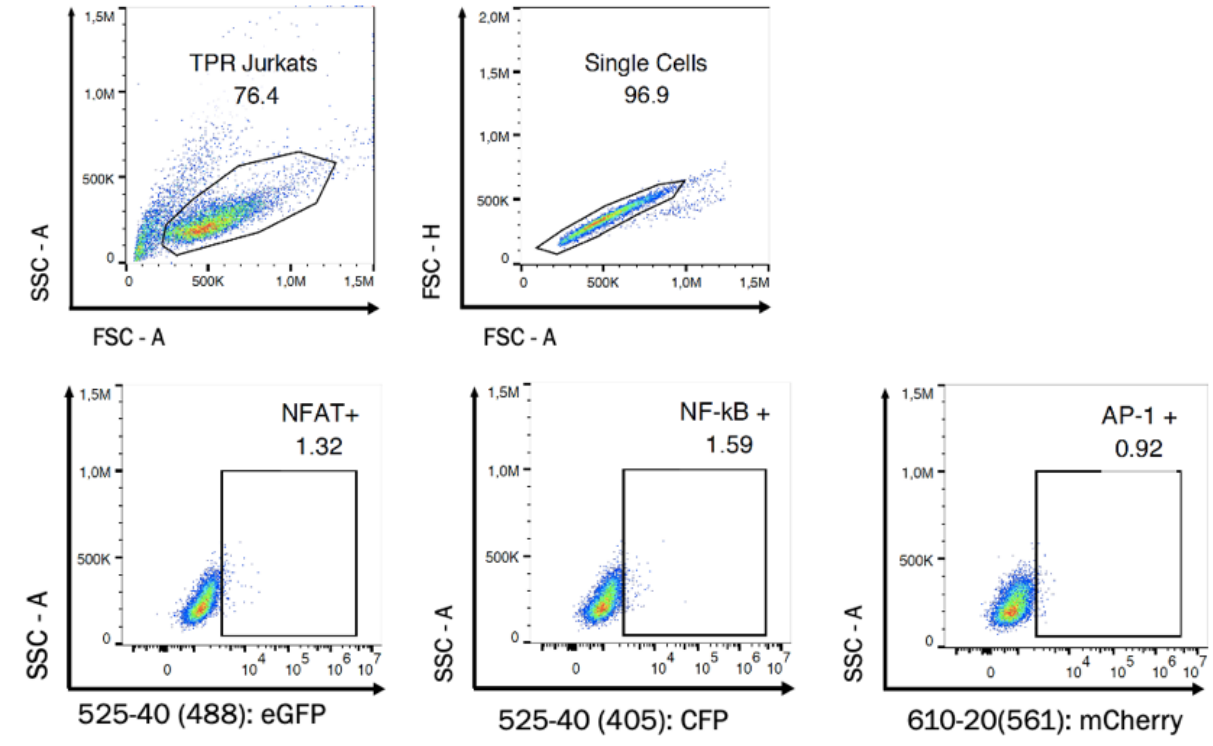

Fig. 3: Gating strategy overview
Flow Cytometry dot plots representing the gating strategy using unstimulated cells (applicable to all TPR stimulation experiments).

and then isolating the single cells within that population by plotting Forward Scatter Area (FSC-A) versus its height (FSC-H). The resulting population were plotted against all three reporter signals versus Side scatter (SSC-A), and positive signal gates were set up based on unstimulated control signal levels (cf. Fig 3). In all samples, the positive signal gates were set up so that cells never exceeded 2.5 % of positive signal in unstimulated conditions.

VIII – Statistical analyses

For figure 6 and 10, statistical analyses were performed using a one-way ANOVA followed by a Bonferroni post-hoc test in Excel (version 16.54). Statistical significance was determined by dividing the alpha number (0.05) by the number of comparisons performed (n): non-significant = $P > 0.05/n$; * = $P \leq 0.05/n$; ** = $P \leq 0.005/n$; *** = $P \leq 0.0005/n$; **** = $P \leq 0.00005/n$. For figure 9, statistical analyses were performed using individual unpaired one-way student's T tests. Statistical significance was determined as follows: non-significant = $P > 0.05$; * = $P \leq 0.05$; ** = $P \leq 0.05/n$; *** = $P \leq 0.05/n$; **** = $P \leq 0.05/n$.

Results

I - In-silico analysis of kinases and phosphatases of the milk EV cargo

With the objective to compile a list of EV proteins which potentially tamper with pathways of T cell activation, an in-silico analysis of the milk EV proteome was performed. Because signaling pathways are generally highly dependent on phosphorylation events, kinases and phosphatases present in the milk EV cargo were focused on. A total of eleven kinases and phosphatases were found in all seven milk EV cargoes of the proteomics data (cf. **Fig**. 4) (van Herwijnen, MJC., et al, [mcp.M116.060426-1, "milk-derived EV"]).

To verify whether these kinases and phosphatases were previously proven to interact with pathways of T cell activation, they were all examined using the Uniprot and PubMed databases. As a result of this detailed investigation, kinases/phosphatases were classified in three main groups: proteins which are unlikely to affect pathways of T cell activation, proteins likely to support T cell activation pathways and proteins likely to inhibit them.

First of all, numerous candidates were selected out as no clear potential interactions were found with pathways of T cell activation. For instance, Alkaline phosphatase tissue-nonspecific isozyme (ALPL) is an enzyme which dephosphorylates SPP1 or osteopontin. Osteopontin expression levels in activated CD4+ T cells are null (Schmiedel, B. J.et al, 2018). Therefore, ALPL was not selected as a promising candidate for milk EV protein-mediated immunomodulation. While Adenylate Kinase 1 (AK-1) is expressed in CD4+ T cells, there is no evidence that it interacts with pathways of T cell activation. Nevertheless, its expression was shown to be reduced by half when T cells were activated. These expression level changes highlight AK-1's role in cellular homeostasis: AK-1 maintains equal Adenosine in different compartments (Schmiedel, B. J.et al, 2018). A hypothesis could emerge suggesting that by increasing AK- 1 levels, EVs shift cells back to a homeostatic state, thus preventing activation. However, no proof was found to support this hypothesis. While YES1 is expressed in T cells, it also could not be linked back to pathways of T cell activation.

Finally, Protein Tyrosine Phosphatase Receptor Type F (PTPRF) was not shown to target any protein belonging to pathways of T cell activation either. UMP/CMP kinase is known to catalyse the phosphorylation of pyrimidine monophosphates, which could not be linked back to pathways of T cell activation.

Then, some milk EV cargo kinases and phosphatases which were found to interact with pathways of T cell activation were classified as likely to support pathways of T cell activation.

Phosphatidylinositol 4 kinase alpha (PI4KA) is an enzyme which kick-starts chains of reactions leading to increase in phosphatidylinositol 4,5- biphosphate (PIP2) production in a wide range of cells (Uniprot), including activated CD4+ T cells (Schmiedel, B. J.et al, 2018). The PIP2 lipid is an essential substrate for enzymes upstream of several T cell activation signaling pathways, such as PI3K and PLC (Di Paolo, G., & De Camilli, P., 2006). Both enzymes contribute to CD28-derived pathways of T cell activation. Therefore, EV-mediated increase in cytosolic PI4KA levels could increase PIP2 biosynthesis and feed into pathways of T cell activation. While no proof exists that PI4KA abundance increases CD28 pathway stimulation, overexpression of PI4KAs was associated with hepatocellular carcinoma and a worse prognosis. This suggests that increased PI4KA leads to the over-activation of proliferation pathways, which can also involve the MAPK and PI3K pathways for example (Ilboudo, A., et al., 2014).

Additionally, PACSIN3 could have been an interesting candidate for inhibition of T cell activation pathways if one of its targets TRPV4 was expressed in activated CD4+ T cells. By inhibiting the TPRV4 calcium channel, which is itself negatively regulated by the calcium pathway, PACSIN3 could have been suspected to inhibit the calcium pathway of T cell activation. However, TPRV4 is not expressed in activated CD4+ T cells (Schmiedel, B. J.et al, 2018). The opposite trend is observed for GLUT1 (highly expressed), PACSIN3's other target. PACSIN3 prevents the internalization of GLUT1 and therefore leads to its accumulation at the cell surface. GLUT1 is a major glucose cellular importer, which is heavily required for T cell activation. Cellular glucose levels were even shown to be the limiting factor in T cell activation, and GLUT1 expression was shown to be CD28-Akt-mTOR pathway dependent (Siska, P. J., et al., 2016 and Jacobs, S. et al., 2008). These results strongly suggest that a PACSIN3-mediated GLUT1 accumulation on the T cell surface could favor T cell activation by providing the glucose necessary for an increased metabolism. Furthermore, higher glucose led to an inhibition of GSK3αβ in GLUT1 transgenic T

cells (Zhao, Y., et al., 2007). As GSK3alpha is a regulator of NFAT export from the nucleus, its reduced activity could lead to T cell activation (Macian, F., 2005).

Kinases/Phosphatases from EV proteomic analysis	Uniprot	Cellular target(s)	T cell activation pathway of the target	Target expression in activated T cells
PTPRJ	Q12913	LAT, ERK, PLC-G1	MAPK, Calcium	Yes
SIRPA	P78324	SHP-1/2	MAPK	Yes
ALPL	P05186	SPP1	N/A	No
PI4KA	P42356	PIP2	PI3K, MAPK	Yes
UMP-CMP kinase	P30085	UMP, CMP, TMP	N/A	Yes
PACSIN3	Q9UKS6	GLUT1	unsure	Yes
AK1	P00568	N/A	N/A	N/A
TAOK1	Q7L7X3	IL-17RA	MAPK	Yes
LYN	P07948	Akt, MEK1/2	MAPK	Yes
PTPRF	P10586	EPHA2	MAPK	No
YES1	P07947	CTNND1	unsure	Yes

Fig. 4: List of kinases and phosphatases found in all 7 milk EV samples used for proteomic analysis (van Herwijnen et al., 2016). This table also includes information regarding which cellular targets the EV proteins interact with, which pathways of interest do these targets belong to and whether they are expressed in activated CD4+ T cells.

Lastly, some milk EV-cargo proteins were classified as potential contributors to the observed inhibited phenotype in CD4+ T cells.

First of all, the receptor-type tyrosine-protein phosphatase eta (PTPRJ) is a phosphatase known to negatively regulate T cell signaling. Expressed in activated CD4+ T cells (Schmiedel, B. J.et al, 2018), PTPRJ mainly dephosphorylates essential proteins of the MAPK pathway, as well as PLC-G1, a central kinase in T cell activation (Zonneveld et al, 2021). Upon EV fusion with the host cell membrane, milk EV PTPRJ was hypothesized to increase the pool of PTPRJ, thus increasing inhibition of pathways of T cell activation.

Furthermore, Signal Regulatory Protein Alpha (SIRPA) is a transmembrane integrin primarily found on myeloid and neuronal cells (Schmiedel, B. J.et al, 2018). By binding to the ubiquitously expressed CD47, SIRPA is known to induce inhibition in macrophages (Gauttier, V., et., 2020). This effect is so potent that tumors upregulate CD47 to inhibit the myeloid cells of the microenvironment (Takimoto, C. H., etal., 2019). The binding of SIRPA leads to the phosphorylation of its intracellular signaling tail, leading to SHP-1 (encoded by PTPN6) and SHP-2 (encoded by PTPN11) sequestration. Because SHP-1/2 are signaling mediators essential to the Ras/ERK pathway, this sequestration reduces cell activation (Feng, G. S., 1999). While SIRPA is not naturally expressed in activated CD4+ T cells, SHP1/2 are (Schmiedel, B. J.et al, 2018). Therefore, if SIRPA-containing milk EVs were to transfer this receptor to the CD4+ T cell membranes, it could be hypothesized that SIRPA engagement would inhibit CD28-derived activation pathways. On the other hand, it could also be hypothesized that EV membrane-bound SIRPA could interact with T cell CD47, which is moderately expressed on activated CD4+ T cells (Schmiedel, B. J.et al, 2018). T cell CD47 stimulation was proven to skew T cell differentiation towards a Th1 phenotype (Bouguermouh, S., et al, 2008). To conclude, while no clear evidence suggests that SIRPA influences T cell activation pathways, the hypotheses put forward support further investigations in SIRPA's role as a milk EV immunoregulator.

Thousand and one kinase 1 (TAOK1) is a serine/threonine kinase mainly involved in the activation of the stress-induced p38/MAPK pathway. At first glance, EV-mediated TAOK1 accumulation in the cell could be expected to feed into p38/MAPK activation. However, it was recently discovered that TAOK1 regulates IL-17-mediated activation by interacting with IL17 receptor A (Zhang Z, et al., 2018). While this was not proven in T cells, activated CD4+ T cells express IL-17RA (Schmiedel, B. J.et al, 2018) and are primary targets of IL-17. By preventing the

formation of the IL-17RA Act-a complex, TAOK1 stimulation was shown to cause a decrease in MAPK pathway engagement and NF-kB translocation to the nucleus. Therefore, EV-mediated TAOK1 increase could potentially contribute to the observed phenotype of lesser CD4+ T cell activation.

LYN is a non-receptor tyrosine protein kinase involved in a wide range of signaling pathways of immunity. Mostly expressed in myeloid cells and B cells, it is barely expressed in T

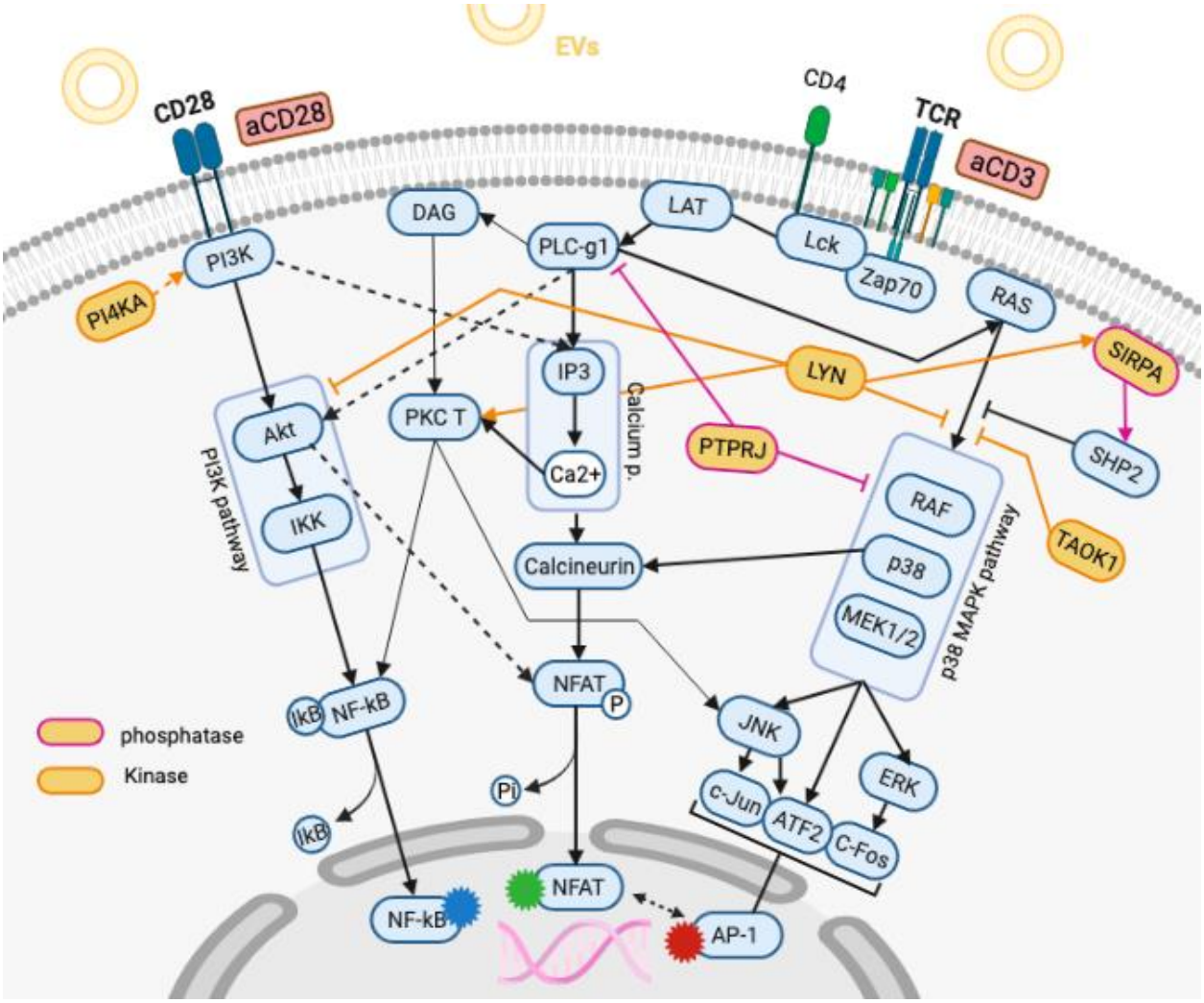

Fig. 5: Scheme representing the milk EV cargo kinases/phosphatases (in orange) identified in the in-silico analysis, and their expected interactions with pathways of T cell activation (in blue).
Made with Biorender.

cells. However, a wide variety of its targets were found in activated CD4+ T cells (Schmiedel, B. J.et al, 2018): Lyn was shown to inhibit CD28-dependent PI3K pathway as well as the TCR

dependent MAPK pathway. It was however also shown to activate the MAPK pathway further downstream, raising doubts as to whether it contributes or reduced T cell activation.

To conclude, within the milk EV kinase and phosphatase cargo, a few proteins were found likely to feed into pathways of T cell activation while others were found likely to have the opposite effect.

II- Optimization of the TPR system for EV-mediated immunomodulation studies

1. Validation of the sensitivity of TPR Jurkat reporters to PMA/Ionomycin.

Before optimization of the TPR read-out system to study milk-EV derived immunomodulation, sensitivity of the reporters had to be confirmed. For this PMA/Ionomycin was chosen as it is a well-known Jurkat stimulus (Klíma, M., et al., 2011) which was previously shown to increase all three reporter levels in the TPR cells (Rosskopf. et al. 2018). Phorbol 12-myristate 13-acetate (PMA) activates Protein Kinase C (PKC) and Ionomycin feeds into the calcium pathway via calcineurin stimulation (**Fig**. S1). Regarding incubation time, it was previously shown that the TPR

Fig. 5: Scheme representing the milk EV cargo kinases/phosphatases (in orange) identified in the in-silico analysis, and their expected interactions with pathways of T cell activation (in blue).
Made with Biorender.

A

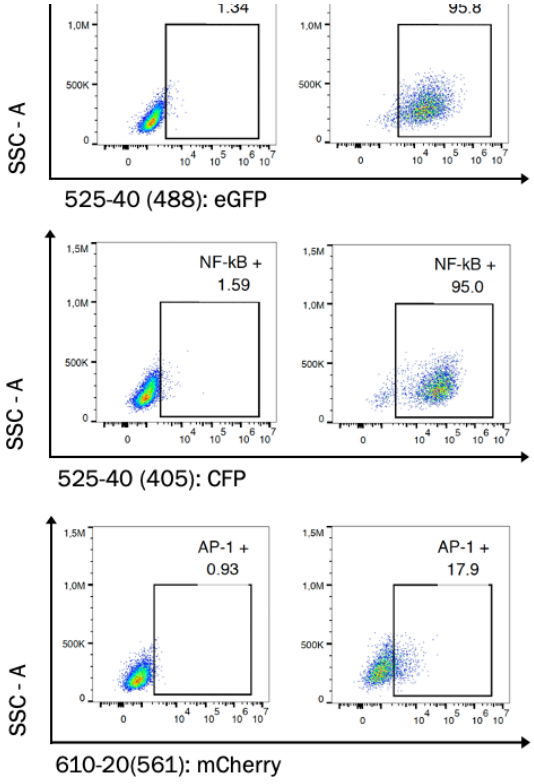

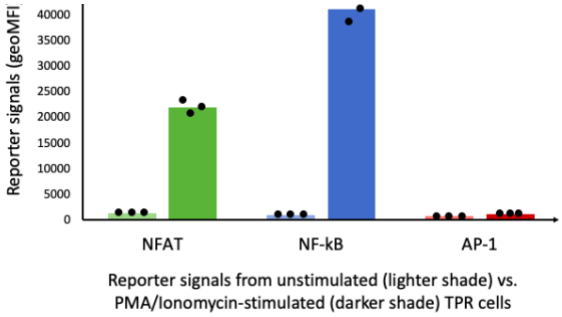

Fig. 6: Testing the TPR system sensitivity through PMA/Ionomycin stimulation.
A: Dot plots of the three reporter signals against Side Scatter (SSC-A) in unstimulated and stimulated conditions. For this, TPR cells were incubated with 0.5 ug/mL PMA and 25 ng/mL of Ionomycin for 48 hours.
B: Geometric Mean Fluorescence Intensity (geoMFI) bar graph of the reporter signals from the same TPR experiment. For each condition, all three technical replicates were included and represented as dots.

reporter signals are more easily measured at 48 hours after stimulation (Rosskopf. et al. 2018). For activation, the TPR cells were thus incubated with 0.5 ug/mL of PMA in combination with 25 ng/mL of Ionomycin for 48 hours. eGFP (NFAT) and CFP (NF-kB) signals were dramatically higher after stimulation with PMA/Ionomycin compared to unstimulated conditions: Both NF-kB and NFAT reporter signal measurements revealed more than 90% of the TPR cells to be gated as positive after stimulation (cf. **Fig** 6A). This data trend was confirmed by the Geometric Mean Fluorescence Intensity (GeoMFI) measured from the same data. Interestingly here, while both NFAT and NF-kB signals increased under stimulation, NF-kB increase was twice that of NFAT (cf Fig. S7). Furthermore, dot plots suggest that NF-kB signal increase in cells forms a positive population separated from a smaller negative population, whereas NFAT is characterized by a whole, gradual population shift (cf. **Fig** 6A). A much lower increase was noted in AP-1 positive cells which represented 18% of the population after stimulation (cf. **Fig** 6B), and close to no increase was observed for AP-1-related GeoMFI.

To conclude, most of the live TPR Jurkat population was shown to emit eGFP-NFAT and CFP-NF-kB reporter signals under PMA/Ionomycin stimulation, with a stronger fluorescent signal for NF-kB. mCherry-AP-1 signal was shown to remain dimly responsive in these stimulation conditions.

2. Investigating the activation potential of anti-CD3 in combination with anti-CD28 antibodies

Now that the TPR cell line reporter sensitivities were assessed, a stimulus that better mimics activation in-vivo and which feeds into CD28-derived pathways was chosen antibodies targeting the CD3 and CD28 molecules (cf. **Fig**. S2). The TPR cells were thus incubated with 2.5 ug/mL of aCD28 in aCD3-coated wells for 8, 24 and 48 hours.

On the one hand, for all three reporters at 48 hours, the percentage of cells gated as positive

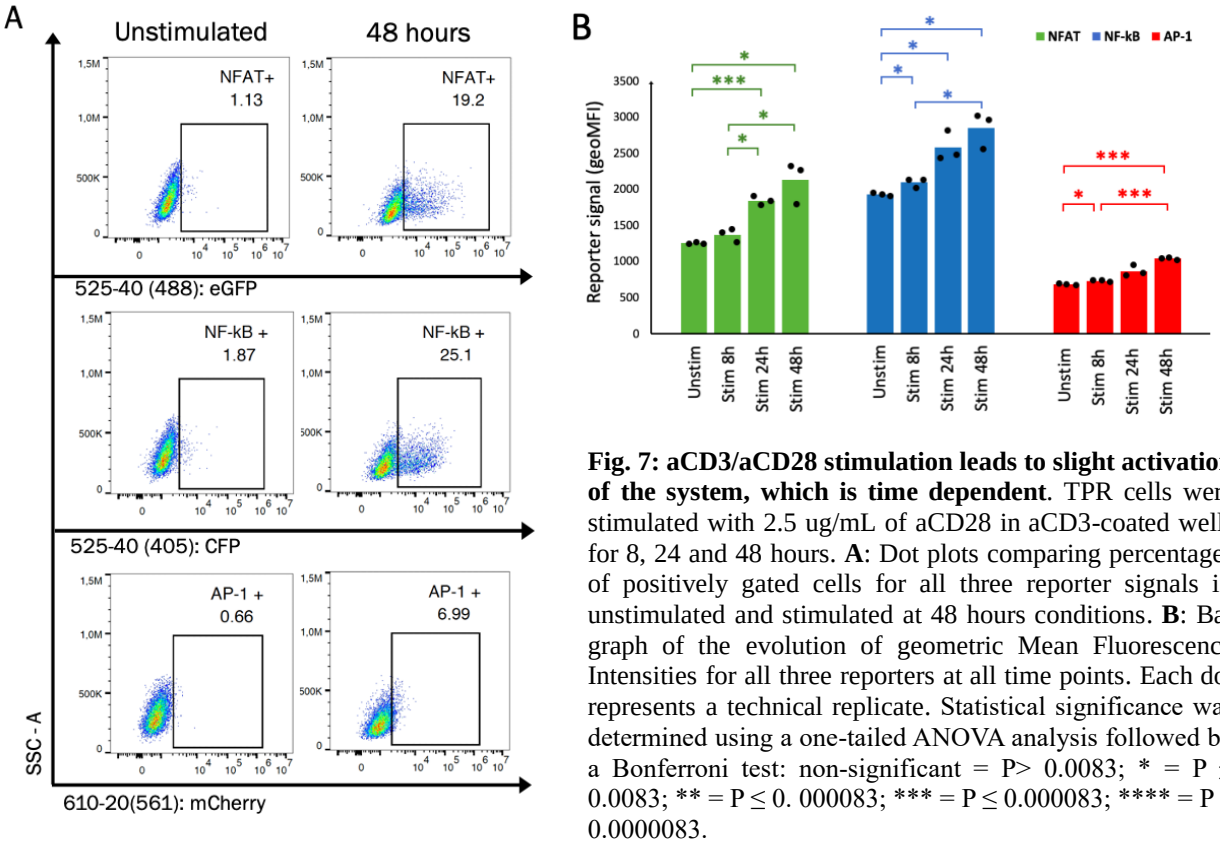

Fig. 7: aCD3/aCD28 stimulation leads to slight activation of the system, which is time dependent. TPR cells were stimulated with 2.5 ug/mL of aCD28 in aCD3-coated wells for 8, 24 and 48 hours. **A**: Dot plots comparing percentages of positively gated cells for all three reporter signals in unstimulated and stimulated at 48 hours conditions. **B**: Bar graph of the evolution of geometric Mean Fluorescence Intensities for all three reporters at all time points. Each dot represents a technical replicate. Statistical significance was determined using a one-tailed ANOVA analysis followed by a Bonferroni test: non-significant = P> 0.0083; * = P ≤ 0.0083; ** = P ≤ 0. 000083; *** = P ≤ 0.000083; **** = P ≤ 0.0000083.

showed an increase after stimulation with aCD3/aCD28. The percentage of positively gated cells increased in a time-dependent manner (cf. **Fig**. S8) until reaching 19% for NFAT, 25 % for NF-kB and 7 % for AP-1 after 48 hours of stimulation. Interestingly, the ratio between different

reporter signals at 48 hours is comparable with PMA/Ionomycin activating conditions (cf. **Fig** 7A). However, this increase was much dimmer than with PMA/Ionomycin

These observations were confirmed by the geoMFI data. Indeed, while the increase of the reporter signals were much lower compared to PMA/Ionomycin, they were statistically significant for all three reporters between unstimulated and stimulated at 48 hours. Furthermore, this increase in reporter signals was time dependent, with 8 hours showing the lowest geoMFI increase and 24 hours an intermediary increase for all three reporters (cf. **Fig** 7B, **Fig** S9).

To conclude, aCD3/acD28 stimulation caused a time-dependent increase in all three reporter signals. Even though aCD3/aCD28 stimulation resembled physiological conditions, it was not chosen as a stimulus for this system optimization as the activation window was too small to study immunomodulation. For future experiments, the 48-hour time point was maintained due to the highest reporter signals found then.

3. Determination of the sub-optimal ConA concentration to obtain strong synergistic effect with aCD28

Because past results suggested that TCR were present in lower amounts on TPR Jurkats compared to non-engineered Jurkats, it was assumed that this was the cause for such a reduced efficacy of stimulation with aCD3/aCD28. Therefore, a CD3 was replaced by a more potent TCR/CD3 stimulant: the lectin Concanavalin A (ConA). This antigen-independent mitogen acts as a primary signal by cross-linking the TCR complex (Ando, Y. et al., 2014).

To pinpoint the sub-optimal concentration of ConA at which aCD28 would provide the strongest added value, a ConA titration at 48 hours was performed on the TPR cells based on concentrations used to activate Jurkat cells in the literature (Gasser, A. et al., 2006; Gómez-

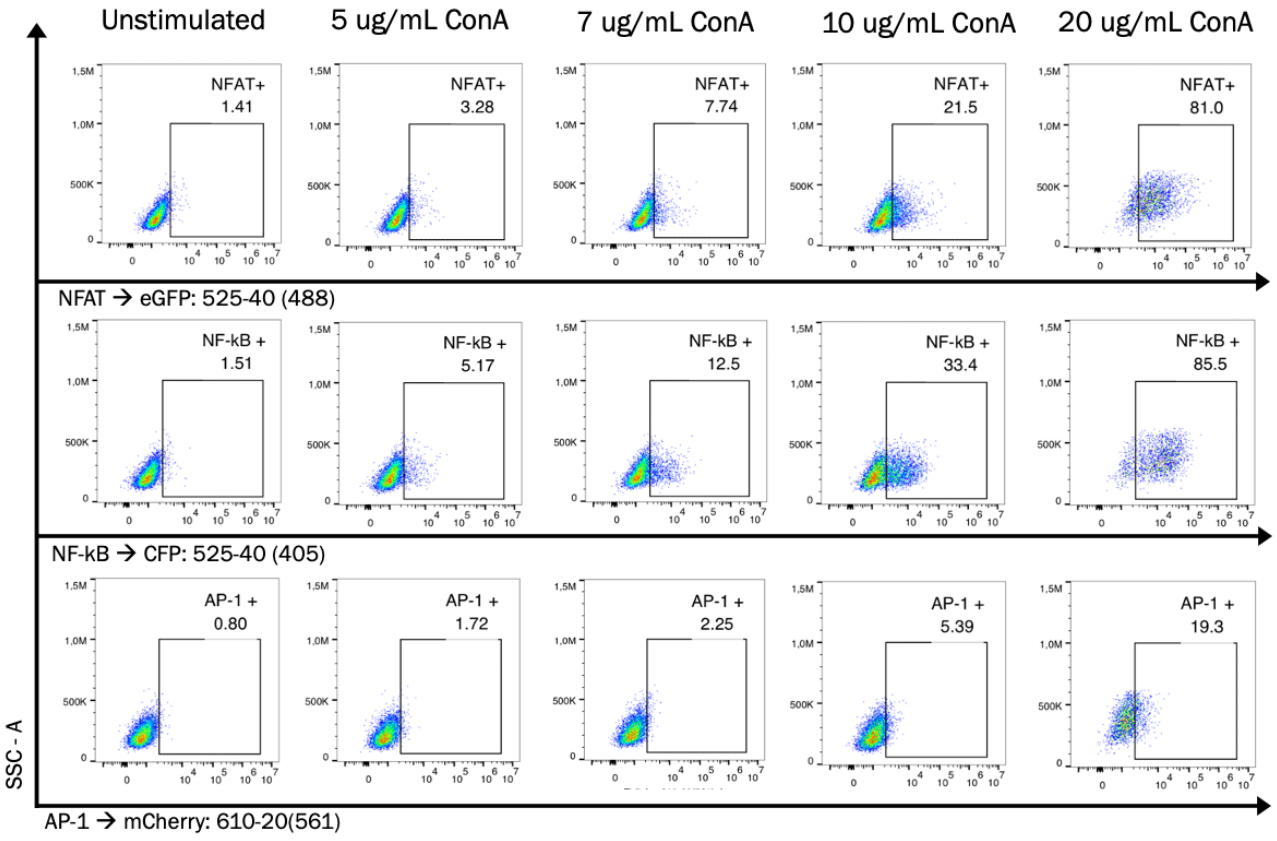

Fig. 8: Effects of ConA titration on the TPR Jurkat cells at 48 hours of incubation
Dot plots representing the percentages of TPR cells gated positively for the three reporters at different ConA concentrations: 5, 7, 10, 20, 40 ug/mL and after 48 hours of stimulation. Dot plots were selected because their percentage values were the median of three technical repeats.

Angelats, M., et al., 2000; Fujita, K., et al., 2019) (cf. **Fig**. 8). In this experiment, it is worth noting that 7 ug/mL, 20 and 40 ug/mL were plated in separate plates from 5 and 10ug/mL samples. These differences were not expected to undermine the results of this experiment as all conditions were identical.

A dose-dependent increase in positively gated cells for all three reporters was observed. For all concentrations, the ratio between reporters was similar to that of the PMA/ionomycin control: strongest for NF-kB and lowest for AP-1 (cf. **Fig**. 8). At 20ug/mL, high reporter signals (more than 80% of cells positive for NFAT and NF-kB reporter signals) were observed. In addition to this, this condition was also characterized by increased cell death: the number of cells in the "Live cells" gate was reduced three-fold from 6000 to 2000. Therefore, 10 and 7 ug/mL were the last tested concentrations of ConA before activation-induced cell death of the TPR population. 10 ug/mL was thus hypothesized as the most sub-optimal concentration to allow for a strong activation when combining it with aCD28.

To conclude, a ConA titration including 5, 7, 10, 20 and 40 ug/mL was performed on the TPR Jurkat cells to determine which ConA concentration would provide a wider window to observe aCD28-derived activation, and the results strongly suggested 10ug/mL of ConA as a concentration candidate.

4. Investigating TPR activation under ConA/aCD28 stimulation

Once a sub-optimal concentration of ConA was selected, the added value of aCD28 to this condition was yet to be tested. The synergistic effect of ConA with aCD28 stimulation is expected to mimic that of in vivo activation by stimulating both CD3 and CD28 derived pathways (cf. **Fig** S3). For this, TPR cells were exposed to 7, 10 and 20 ug/mL of ConA with and without 2.5 ug/mL of aCD28 for 48 hours. The 7 and 20 ug/mL conditions were added to provide an upper and lower frame to the selected concentration of 10 ug/mL. It is worth noting that the 20 ug/mL results were recorded in a different experiment compared to other conditions. With the only difference being cell passage count, this discrepancy was assumed to have very little impact on comparability of the results.

As expected from conclusions of the ConA titration, the addition of aCD28 to 7ug/mL of ConA did not cause signal increase for any reporter. AP-1 reporter signal did not increase under any circumstances. However, for NFAT and NF-kB, the percentage of positive cells increased when aCD28 was added to 10 and 20 ug/mL of ConA. Interestingly, the number of cells represented by the height of the histogram curves drastically decreased for all three reporters at 20 ug/mL of ConA + aCD28 compared to 10ug/mL of ConA + aCD28. The data thus confirms what was hypothesized from the ConA titration: 7ug/mL was too low of a ConA concentration to allow aCD28 stimulation to amplify the activation signal, and 20 ug/mL of ConA with aCD28 provoked Antigen Dependent Cellular Cytotoxicity (ADCC). This is also clearly noticeable on dot plots formats (cf. **Fig** S10) It was thus confirmed that 10 ug/mL + 2.5 ug/mL was an ideal activating condition for immunomodulatory studies on CD28 derived pathways (**Fig**. 9A).

An analysis of the added value of aCD28 on these ConA concentrations was carried out using the geometric Mean Fluorescence Intensity (geoMFI) of the NFAT, NF-kB and AP-1 reporter signals. To determine the aCD28 added value in reporter signals, the geoMFI of the ConA only controls were subtracted to the values obtained from respective ConA with aCD28 samples. Then, the resulting numbers were divided by the geoMFI from the ConA only controls, and the whole was multiplied by 100 to obtain percentage of signal increase. For the NFAT signal, both 10 and 20 ug/mL underwent a comparable signal increase of 60% when adding aCD28. Moreover, NF-

kBrelated geoMFI increased by 180% when aCD28 was added to 10 ug/mL of ConA, compared to 126.5 % at 20 ug/mL of ConA. Finally, AP-1 signal exhibited stronger increase at 20 ug/mL of ConA, with an MFI increase of 28.5 %, rather than 11.75% at 10ug/mL. All reporter signals showed lower increase at 40ug/mL conditions (cf. **Fig**. 9B).

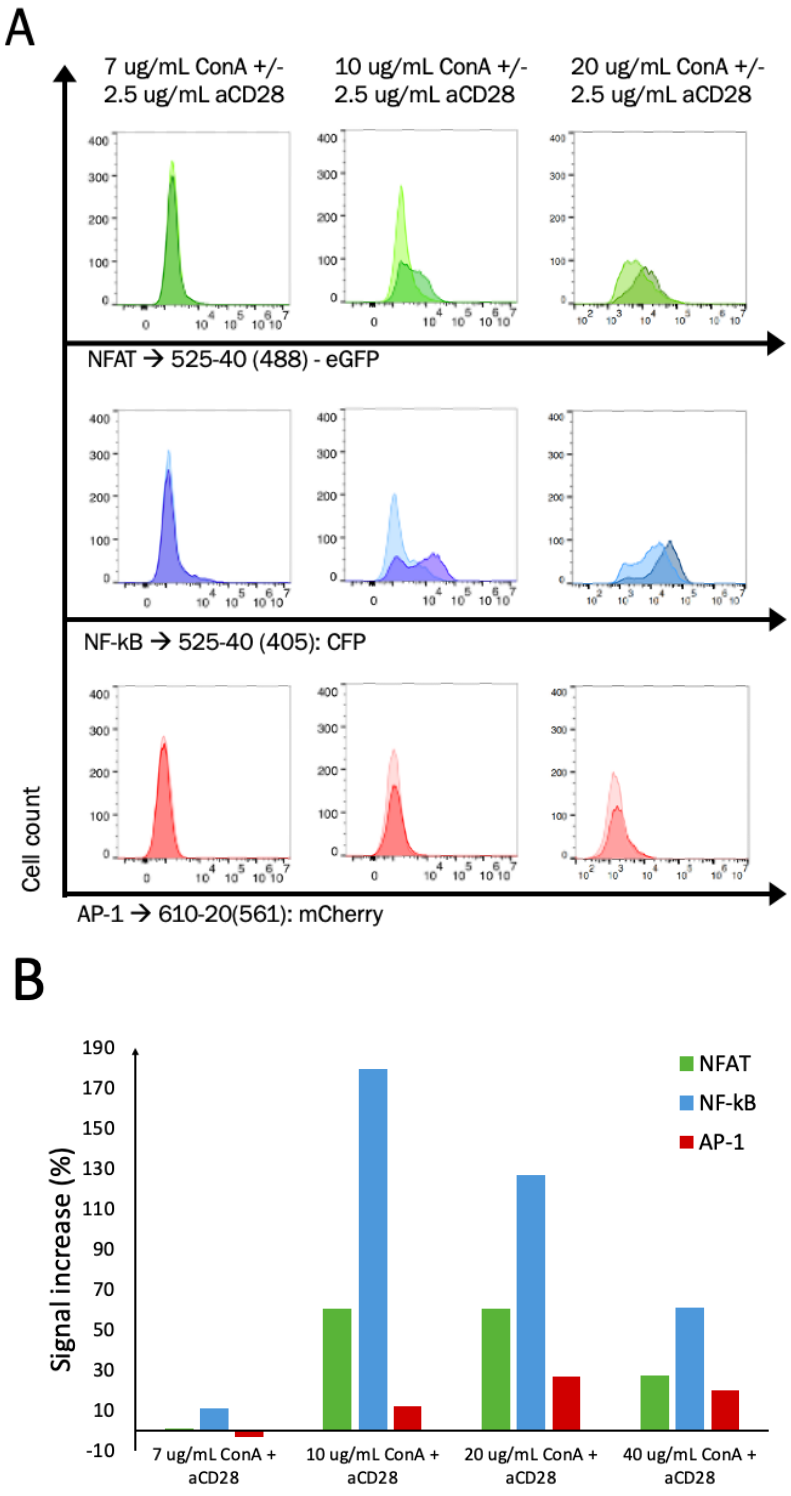

Fig. 9: Investigation into the added value of 2.5 ug/mL of aCD28 to ConA-dependent TPR activation.

A: Histogram overlays of all three reporter signals contrasting ConA stimulation with or without added aCD28. Signal curve from ConA only data is represented in lighter shade whereas the curve for ConA with aCD28 is colored with a darker shade. All results were measured in triplicate, and the median data sets were used here. This data is also accessible in a dot plot format (cf. **Fig**. S10).

B: Bar graph representing the aCD28-related geometric Mean Fluorescence Intensity (geoMFI) increase (in percentages) for 7, 10, 20, and 40 ug/mL of ConA, per reporter. The percentages were obtained by subtracting ConA+aCD28 values to ConA only values. Then this number was divided to ConA only values, and the total was multiplied by 100. All values used were averages of technical replicates. The geoMFI data used to generate this figure is available (cf. **Fig**. S11).

To conclude, 10ug/mL in combination with 2.5 ug/mL of aCD28 proved to provide the widest activation window to study aCD28 derived activation in this TPR system while still avoiding activation induced cellular toxicity. The NF-kB reporter signal was particularly impacted by aCD28 addition.

III - Validating the sensitivity of the optimized TPR system to EV-mediated inhibition

1. Measurement of the immunomodulatory effects of milk EVs on stimulated TPR Jurkats

To validate whether the optimization of the TPR Jurkat read-out system allows detection of milk EV-derived immunomodulation, TPR Jurkat cells were stimulated for 48 hours in EV-containing medium from three donors and their respective EV isolation procedural control called EV depleted samples. To measure the extent at which milk EVs target CD28-derived pathways, the EV-exposed TPR cells were stimulated with 10 ug/mL of ConA and 2.5 ug/mL of aCD28 or with 10 ug/mL of ConA only. As a control for the potential activating effects of EV samples themselves on the cells, unstimulated samples were also exposed to the EV and EV depleted samples.

For the TPR cells which were exposed to 10ug/mL of ConA without aCD28, EVs from all three donors led to a statistically significant reduction in reporter geoMFI values (cf. **Fig**. 10). The activation signal for the ConA-activated cells exposed to EV depleted procedural controls showed a lesser inhibition than their EV counterparts, without completely reaching positive control levels. The only exception was NFAT, which showed non-significant differences between ConA stimulation and ConA + EV depleted population geoMFIs. For AP-1 and NF-kB, the statistical significance between these conditions was also reduced but still notable. Overall, this data suggests that cells stimulated with 10ug/mL of ConA without aCD28 are inhibited in the presence of milk EVs.

For TPR cells treated with 10ug/L of ConA in combination with 2.5 ug/mL of aCD28, similar trends were observed at a different magnitude. As previously shown, adding aCD28 to ConA drastically increased reporter signal values except for AP-1. Indeed, NFAT reporter values were increased, and NF-kB reporter values tripled upon aCD28 addition. EVs decreased TPR cell NFAT signal by half, almost back to unstimulated levels (cf. **Fig**. S12). Similarly, EV led to a 4-fold decrease in NF-kB signal, back to unstimulated levels: from 6000 to around 1500 (cf. **Fig** S13). Finally, AP-1 signal in the presence of EVs also slightly decreased back to unstimulated levels:

from 1250 to 900 (cf. **Fig**. S14). For all reporters, EV depleted procedural controls also led to a

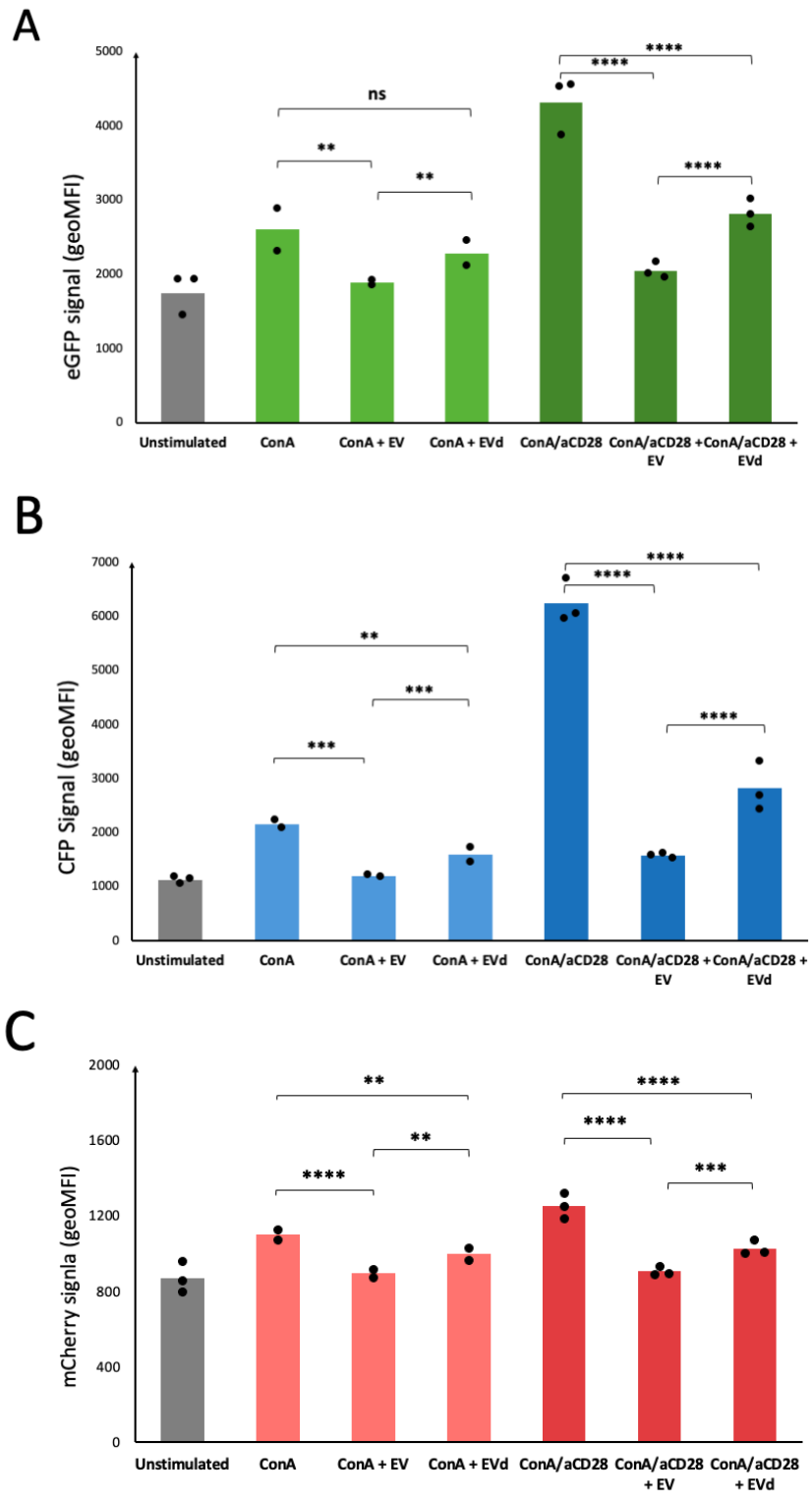

Fig. 10: Comparing the inhibitory effects of milk EVs from three donors and their EV depleted controls on cells stimulated with 10ug/mL of ConA and 10ug/mL of ConA with 2.5 ug/mL aCD28. TPR cells were incubated for 48 hours. **A**: Bar graph of the NFAT reporter (eGFP) geoMFI. **B:** Bar graph of the NF-kB reporter (CFP) geoMFI. **C:** Bar graph of the AP-1 reporter (mCherry) geoMFI. For non EV-containing conditions, each dot represents an average of the technical triplicates of one experiment, and for conditions including EVs, each dot represents an average of three biological replicates (donors) for each experiment (2 experiments for ConA and 3 for ConA+aCD28). Statistical significance was determined as follows: non-significant = $P > 0.05$; * = $P \leq 0.05$; ** = $P \leq 0.01$; *** = $P \leq 0.001$; **** = $P \leq 0.0001$.

statistically significant decrease but to a lesser extent than EV-exposed cells. For instance, the NF-kB reporter GeoMFI value was 2500 in EV-depleted-exposed TPR cells, only 1000 units higher than cells exposed to EVs. For AP-1, the EV-depleted conditions led to a geoMFI of 1000, only 100 units higher than unstimulated conditions (**Fig**. 10 A, B, C).

Overall, EVs were shown to cause a reduction in the three reporter signals, with a strongest effect on NF-kB, a strong effect on NFAT and lower but still significant effect on AP-1. While this effect was much stronger under ConA/aCD28 stimulation conditions, it was also observed for cells treated with only ConA stimulation.

2. Testing the TPR system for measurement of differential milk EV-mediated immunomodulation.

With The TPR read-out system optimized to measure milk EV mediated inhibition, it was further tested with more complex milk EV samples. The TPR Jurkat cells were here again stimulated with 10 ug/mL of ConA and 2.5 ug/mL of aCD28 for 48 hours, in presence and absence of milk EVs. The effects of milk EVs from six healthy donors were compared to those of milk EVs from six allergic donors.

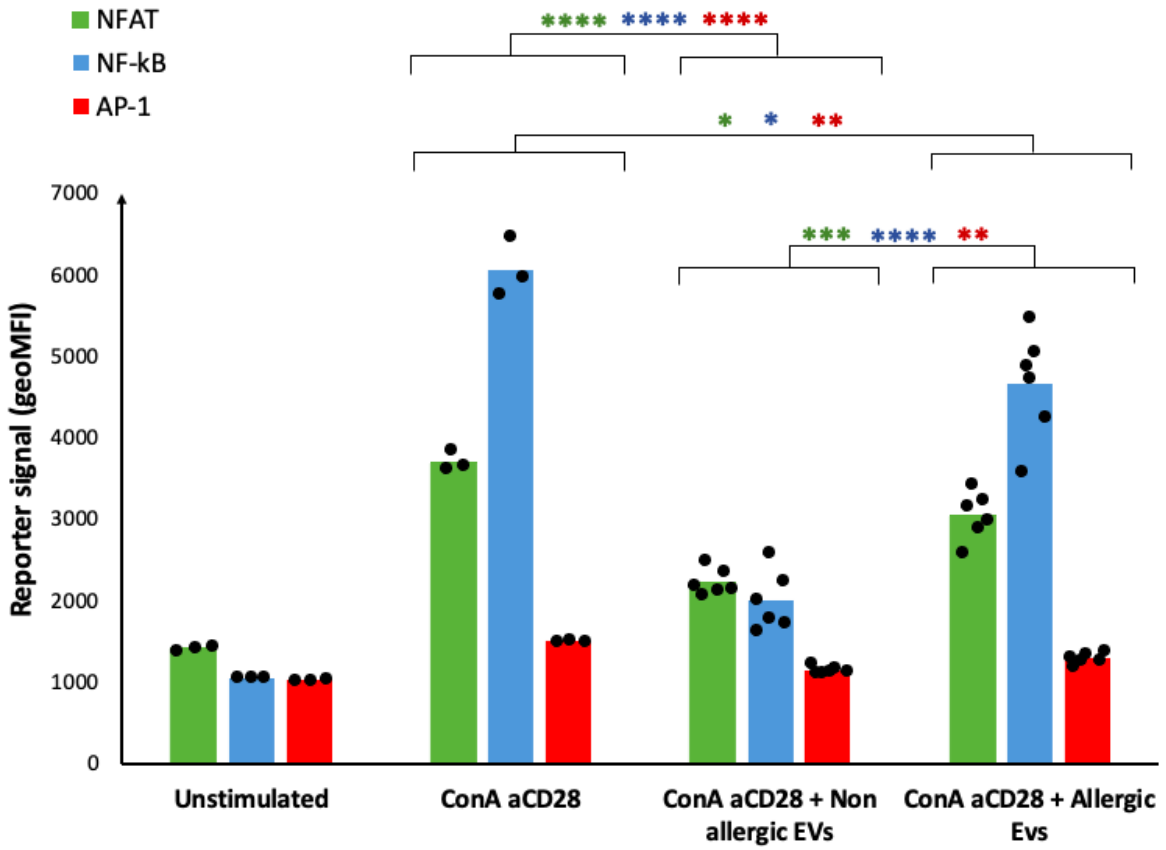

Fig. 11: GeoMFI bar graph validating the TPR Jurkat read-out system through the measurement of differential immunomodulation between milk EVs from healthy donors and milk EVs from allergic donors. TPR cells were incubated for 48 hours with 10 ug/mL of ConA and 2.5 ug/mL of aCD28, in the presence/absence of allergic or non-allergic EVs. Each dot represents one measurement. Unstimulated and stimulated conditions were measured in technical triplicates. Milk EV from six allergic and six non-allergic donors were used for the EV-related conditions (six biological replicates for each). Averages of the geoMFIs from the replicates of each condition were used to create the bars. Statistical significance was determined as follows: non-significant = P> 0.0083; * = P ≤ 0.0083; ** = P ≤ 0.00083; *** = P ≤ 0.000083; **** = P ≤ 0.0000083.

Here again, the synergistic effect of ConA with aCD28 increased the signals (geoMFI) of all three reporters, particularly that of NF-kB and NFAT. Also, all six samples from healthy donors caused a significantly lower increase in reporter signals, particularly for NF-kB. However, EVs from allergic donors were much less capable of inhibiting TPR activation. Indeed, the NF-kB reporter signal for activated TPR cells exposed to allergic EVs was twice that of cells exposed to healthy EVs. The differences between allergic EV-exposed TPR cells and the positive controls were still statistically significant though.

To conclude, The TPR system was able to prove that milk EVs hold different inhibitory effects on pathways of Jurkat cell activation based on whether they come from allergic or non-allergic patients. Milk EVs from allergic patients were not as potent in reducing ConA with aCD28-mediated activation as healthy EVs. Furthermore, the NF-kB reporter signal is the most sensitive to ConA with aCD28 stimulation and milk EV modulation. Finally, this experiment validated the TPR system's capacity to detect differential immunomodulation of activation signaling pathways.

III. Comparing amounts of kinases and phosphatases of interest in EV cargoes from allergic and non-allergic donors.

Given the significant differential inhibitory effects of milk EVs from allergic and non-allergic donors, an analysis previously performed to compare the proteome of milk EVs from allergic and healthy donors was studied. The milk EV cargo phosphatases and kinases which were previously (cf. I 1) classified as potential inhibitors, supporters, or bystanders of pathways of T cell activation were looked for within the allergic versus non allergic proteomic comparison. This analysis was performed in the hopes of validating the in-silico kinase/phosphatase candidates by mirroring changes in proteomic composition and observed phenotype. Within the 11 proteins of the in-silico list, only 6 proteins were found in at least 60% of either allergic or non-allergic samples. PI4KA, UMP/CMP kinase, PACSIN3, LYN and YES1 were present in all allergic and non-allergic EVs in similar amounts. It was thus quite unlikely that they are responsible for the observed differences.

Discussion

CD4+ T cell activation was shown to be reduced in the presence of human milk EVs. However, it is not yet understood the exact mechanisms by which EVs increase threshold for T cell activation. While certain microRNAs were proven to silence the expression of genes required for activation, the observed prevention of T cell activation was immediate, suggesting that other milk EV components mediated this effect via interference with signaling pathways of T cell activation. In parallel, the milk EV proteome seemed to include a wide range of candidates potentially interfering with pathways of T cell activation. It was thus hypothesized that milk EV proteins might contribute to the observed immediate reduction in T cell activation, with particularly strong interference with CD28 signaling.

The first step in investigating the link between milk EVs and T cell activation involved an in-depth analysis of the milk EV proteome from healthy donors, and in particular the kinases and phosphatases which are likely to interfere with phosphorylation and dephosphorylation events regulating most of the signaling cascades in T cell activation. As a result of this in-depth investigation in the established targets of the selected enzymes, they were classified as: unlikely to interfere with T cell activation pathways, likely to support T cell activation signaling or likely to inhibit T cell activation signaling. Interestingly, the results presented a balanced mix of candidates for both the activation and inhibition of T cell activation pathways. Because the proteins are most likely not the only components of milk to cause this immediate effect, it is not yet known whether the proteome itself is inhibitory. What can safely be concluded from this analysis, is that if the milk EV proteome is indeed a main driver of the observed reduced activation, the kinases and phosphatases hypothesized to inhibit the pathways are very likely to be contributing to this mechanism.

Activation Signaling is particularly difficult to investigate in primary T cells, due to culturing challenges and low percentages of T cell activation in response to stimuli. Therefore, a read-out system for the stimulation of major signaling pathways of activation was required. The activation conditions of a Triple Parameter Reporter Jurkat cell line were thus optimized to study

EV-mediated immunomodulation on three major pathways of T cell activation. The sensitivities of the system reporters were first assessed using the established Jurkat stimulus: PMA and Ionomycin. As a result of the stimulation of three main pathways of T cell activation by PMA/Ionomycin, an increase for all three reporter signals was expected as demonstrated by the team which engineered the TPR cell line (Rosskopf et al., 2018). However, while NFAT and NF-kB reporter signals dramatically increased upon stimulation, the AP-1 reporter (mCherry) signal remained low. Although AP-1 reporter signal was responsive to stimulation and immunomodulation in all other experiments involving the TPR system, mCherry signal always remained low, making it difficult to detect immunomodulatory effects or establish statistical significance. These results are not in line with numerous studies, which have established AP-1 as a marker of Jurkat cell activation (Rincon, M., & Flavell, R. A., 1994). mCherry might be harder to detect by Flow cytometry, which could be the reason for a reduction in signal measurement. This observed loss of AP-1 reporter sensitivity could be caused by faulty TPR cells themselves.

After assessing the reporter sensitivities, the first stimulus to be tested on the TPR cells was chosen based on its resemblance to T cell stimulation in-vivo: anti-CD3 and anti-CD28 antibodies. These stimuli were expected to provide a potent time-dependent increase in all three reporters. aCD3/aCD28 stimulation-dependent increase in all three reporters were in fact statistically significant between unstimulated and cells stimulated for 48 hours. 48 hours was thus chosen as a reference time point for all experiments to follow. The increase in signal was much lower than what was shown in other studies. This could be due to a wide range of factors. However, the previously observed strong PMA/Ionomycin stimulation avoids the surface CD3 and CD28 by stimulating the same pathways at a more downstream node (cf **Fig** S1). The cause of reduced activation with aCD3/aCD28 was thus expected to be linked to CD3 or CD28. Furthermore, a quantification of endogenous CD3 levels on the TPR cells was previously performed and had found lower levels compared to other Jurkat cells [data not published].

As a well-known potent stimulator of CD3, ConA was chosen as a replacement for aCD3. The first step in setting up a strong ConA and aCD28 synergistic stimulation of the TPR system involved identifying a sub-optimal activating concentration of ConA to which aCD28 could be added. The added value of a constant concentration of aCD28 in activating the TPR cells was

studied on varying concentrations of ConA. While the strongest added value of aCD28 for the AP-1 signal was observed at 20 ug/mL of ConA, the added value of aCD28 for NF-kB signal was much higher at 10ug/mL. Considering that the experiment objective was to prioritize immunomodulatory effects on the CD28 derived pathways (i.e. represented by NF-kB activity) (cf. **Fig** 1), 10ug/mL was the chosen condition.

The TPR cells confirmed the hypothesis that the milk-EV-mediated inhibition occurs via targeting of the signaling pathways of T cell activation. Within the TPR system, a reduced fluorescent signal means that translocation of the corresponding transcription factor was reduced, and therefore that the signaling pathways leading to this translocation were interrupted. While all three reporter signals were significantly reduced in presence of EVs in cells activated using 10 ug/mL of ConA and cells activated using 10ug/mL of ConA with 2.5 ug/mL of aCD28, the effect was much stronger in the case of added aCD28. Furthermore, the effect was also much stronger for the NF-kB signal compared to AP-1 and NFAT, a signal canonically considered to be mediated by CD28-derived pathways. While it is tempting to use these observations to support the hypothesis that milk EVs primarily affect CD28 pathways, it might not be straight-forward. NF-kB is the most sensitive reporter of the TPR system for all tested stimulation, and it is difficult to say whether a greater impact on NF-kB reporter signal is caused by more EV protein targeting or just better sensitivity. Finally, it is difficult to compare EV effects on 10 ug/mL ConA only versus ConA with aCD28 conditions because 10ug/mL of ConA is a sub-optimal concentration which was selected to work synergistically with aCD28. Therefore, the “ConA only” at 10 ug/mL condition might not be stimulating the TPR cells enough to observe proper immunomodulation. Overall, thanks to stronger statistics for ConA+aCD28 and a sharper effect of EVs on NF-kB reporter signaling in ConA + aCD28 activation conditions, it can be safely stated that EVs are likely to primarily focus on CD28-derived pathways, while still affecting TCR-derived pathways too.

Later, the ConA/aCD28- activated TPR system was validated by detecting differential EV-mediated immunomodulation between samples from allergic and samples from non-allergic parents. Even though the criteria used to consider a donor as allergic were diverse (cf. **Fig** S4**),** the observed effect over all 6 biological replicates was unanimous: EVs from allergic donors are

significantly less inhibitory compared to those of healthy donors. EVs play a major role in mediating allergy between the cells of an individual (Alashkar Alhamwe, et al., 2021). Furthermore, T cells differentiation and activation is strongly associated with allergy (Wambre, E., et al., 2012; Smart, J. M., & Kemp, A. S., 2002). Therefore, because allergy is a type of deregulated immunity, allergic EVs could be contributing to allergy development by failing to regulate CD4+ T cells. In addition to this, the T cell CD28 co-receptor engagement was defined as a crucial step in pathogenesis of asthma (Jaffar, Z. H., et al., 1999; Larché, M., et al., 1998). This highlights the potentially vital impact of healthy milk EVs in avoiding allergy development by primarily targeting CD28-derived pathways. It would thus be interesting to investigate whether the EVs found in milk resemble the profile of those maintaining allergy within an individual. If these EVs turn out the share the same profile, this could be an explanation for the observed reduction in inhibitory capacities of milk EVs from allergic donors. Interestingly, in the case of breastfeeding from an allergic parent to an infant, these milk EVs could also potentially fail to maintain tolerance of the infant's gut immunity. This could indirectly contribute to the development of allergies in the infant.

As expected, the EV-depleted procedural controls exhibited lowered capacities to decrease T cell activation in both ConA only and ConA with aCD28 activating conditions. However, EV depleted samples also always led to significant decreases in reporter signals compared to activated cells. There are different potential explanations for this. For example, as the EV depleted procedural control consists of the supernatant left after gradient ultracentrifugation, perhaps some EVs were left there. This observed inhibition in the presence of the EV-depleted controls could be caused by unknown other immunomodulatory components of milk which remained in the supernatant. Finally, this could be caused by immunomodulatory agents added within the EV isolation process. If this is the case, then milk EV samples contain the exact same components as they were processed in identical manners, making EV and EV depleted differences reliable. To conclude, it might be difficult to pinpoint exactly what could be contributing to this strong inhibitory effect of the EV-depleted procedural control samples. However, the differences between EV-depleted- and EV-treated activated cells are still significant, suggesting that the majority of the inhibition can be attributed to EVs.

Overall, the TPR system provides very sensitive measurements of T cell activation. The strength of this system also arises from its practicality: TPR cells are easy to store, culture and measure. No staining is required prior to flow cytometry. Finally, they are much more responsive to activation, with up to more than 90% of cells gates positively for NF-kB signal with PMA/Ionomycin compared to around 40% with primary cells.

On the other hand, the TPR cells are derived from a Jurkat cell line, which implies non-negligible differences with primary T cells such as higher expression of key nodes in pathways of activation (Bartelt, R. R., et al., 2009). Due to this difference in robustness of activation pathways, activated T cells could be even more sensitive to EV modulation than Jurkat. as their activation levels Additionally, it is important to remember that the three transcription factors measured in the system are not representative of all the pathways of T cell activation, and that the activation landscape is much more complex than that.

The in-silico analyses of the milk EV proteome and the optimization of the TPR cell system could be enhanced in multiple ways.

First of all, it would be a good idea to re-investigate the impact of milk EVs on TPR cell activation in ConA only versus ConA with aCD28 conditions, but with a stronger ConA only stimulus this time. This would lead to more comparable activation strength between the two conditions, and hopefully provide a better understanding of whether EVs are more likely to affect CD28 derived pathways or not.

The issue of low AP-1 reporter sensitivity could be caused by impaired detection of the signal by flow cytometry. An attempt to observe the signal via fluorescence microscopy could help check this. If the signal appears strong at the microscope, this would be a confirmation that the TPR works well and that the issue relies in measurement complications. Because the TPR reporter fluorophores are not expressed bound to the transcription factors themselves but are rather upregulated as a response to TF binding to its RE (Jutz., et al., 2016), microscopy will not inform us of the localization of TF in the cell at all. However, quantification of the signal will very strongly represent levels of TF translocation (i.e. activation), just as it did with flow cytometry.

Regarding the in-silico analysis, it would be interesting to expand the systematic selection to more members of the milk EV proteome. The current list only includes kinases and phosphatases which were detected in all seven EV samples used for proteomics. In this approach, promising

kinase/phosphatase candidates might have been missed if they were not detected in 100% of the samples. Looking at those expressed in most samples but not all could increase the list size. While it is less likely, non-kinases/non-phosphatases might also directly interfere with pathways. Expanding the research towards other protein families could also be fruitful. Furthermore, there is a possibility that EV proteins interact and support inhibitory pathways such as PD-1 resulting pathways. Performing a similar in-silico analysis on inhibitory pathways in the hopes of finding strong supporting proteins would be recommended.

The TPR system is a strong tool to obtain general understanding of immunomodulation of signaling pathways. Comparing the immunomodulation of the same element in differently activated TPR could inform us a lot on the pathways targeted by this element. For example, in the case of milk EVs, testing their effects on PMA/Ionomycin-activated cells could inform us about whether EVs interact upstream or downstream of the pathways of interest. This is because PMA and ionomycin stimulate the same pathways as ConA and aCD28 but start feeding into them at a much downstream node (cf. **Fig**. S1). A reduction in inhibitory effects with PMA/Ionomycin could strongly suggest that the EV effects are intervening at a more upstream node of the pathway. Similarly, synthetic drugs could also be used to block certain pathways and test whether immunomodulation still occurs or changes.

Although this project clearly demonstrated that milk EVs target pathways of T cell activation, a causal link between the milk EV cargo proteins and this observed inhibition has yet to be established.

The phosphorylation states of various targets of selected kinase and phosphatase candidates from the in-silico analysis (PTPRJ, SIRP-Alpha) could be measured in presence and absence of milk EVs. An increase or decrease in phosphorylation would establish a causal link between the EV proteome and this phosphorylation event, thus strongly suggesting that the investigated candidate mediated this change. Measurement could be performed using phospho-western blotting on TPR cells selected using Fluorescence Activated Cell Sorting (FACS) to increase result quality and avoid unresponsive cells. On a larger scale, phospho-proteomics could also be performed to compare phosphorylation events of a much wider range of proteins in presence and absence of milk EVs.

Other experiments could also further investigate the potential effects of the EV cargo proteins on T cell activation. For instance, a synthetic vesicle-building approach could be adopted to recreate a milk EV in a controlled manner (Fernandez-Trillo, F., et al., 2017; Eytan. G. D., 1982). By controlling the composition of the system, causal identification of specific immunomodulatory components could be established using the TPR system (for example – adding only one candidate of interest, or the proteome isolated from other milk EV components).

To conclude, with a list of promising milk EV protein candidates to investigate and an optimized read-out system to measure Jurkat activation of pathways of interest, the road towards the establishment of a causal link between specific proteins of the milk EV cargo and the inhibition of T cell activation has progressed. Unravelling specific mechanisms of milk EV-mediated T cell immunomodulation contributes to knowledge gathering on the importance of human milk EVs in immune regulation of the newborn's mucosal immunity. Regulation of infant adaptive immunity in the first months of life is a decisive factor in healthy gut immunity and microbiota development. In parallel, studying the potential differences of milk EV compositions in health and disease (allergy) could contribute to better defining and identifying a healthy milk. Taken together, these understandings could help enhance medical advice in breastfeeding, improve milk formulae or supplements which would all lead to a healthier infant development.

Acknowledgements

I would like to extend my deepest gratitude to my examiner Prof. Marca Wauben and daily supervisor Alberta Giovanazzi for this opportunity and their supportive and valuable feedback.

I would also like to thank all members of the Division of Cell biology, Metabolism and Cancer, especially Marije Kleinjan and Martijn van Herwijnen for their daily insights and guidance. Special thanks to Judith Neve for her advice on statistical analyses.

Finally, this journey would not have been possible without those who provided me with unconditional support: Petri de Jager, Victor Dueñas Otero, Vaishnervi Manoj, Ilaria Nesi, Lonneke Broeks, Jessica Tamiazzo, Njeri Ndungu, Caroline Vincelot, Pascal Vincelot and Julien Vincelot.

References

- Alashkar Alhamwe, B., Potaczek, D. P., Miethe, S., Alhamdan, F., Hintz, L., Magomedov, A., & Garn, H. (2021). Extracellular vesicles and asthma—More than just a co-existence. *International Journal of Molecular Sciences*, *22*(9), 4984.
- Ando, Y., Yasuoka, C., Mishima, T., Ikematsu, T., Uede, T., Matsunaga, T., & Inobe, M. (2014). Concanavalin A-mediated T cell proliferation is regulated by herpes virus entry mediator costimulatory molecule. *In Vitro Cellular & Developmental Biology-Animal*, *50*(4), 313-320.
- Andreas, N. J., Kampmann, B., & Le-Doare, K. M. (2015). Human breast milk: A review on its composition and bioactivity. *Early human development*, *91*(11), 629-635.
- Bartelt, R. R., Cruz-Orcutt, N., Collins, M., & Houtman, J. C. (2009). Comparison of T cell receptor-induced proximal signaling and downstream functions in immortalized and primary T cells. *PloS one*, *4*(5), e5430.
- Bouguermouh, S., Van, V. Q., Martel, J., Gautier, P., Rubio, M., & Sarfati, M. (2008). CD47 expression on T cell is a self-control negative regulator of type 1 immune response. *The Journal of Immunology*, *180*(12), 8073-8082.
- Chan, A. C., Iwashima, M., Turck, C. W., & Weiss, A. (1992). ZAP-70: a 70 kd protein-tyrosine kinase that associates with the TCR ζ chain. *Cell*, *71*(4), 649-662.
- Claud, E. C., & Walker, W. A. (2001). Hypothesis: inappropriate colonization of the premature intestine can cause neonatal necrotizing enterocolitis. *The FASEB Journal*, *15*(8), 1398-1403.
- Di Paolo, G., & De Camilli, P. (2006). Phosphoinositides in cell regulation and membrane dynamics. *Nature*, *443*(7112), 651-657.
- Feng, G. S. (1999). Shp-2 tyrosine phosphatase: signaling one cell or many. *Experimental cell research*, *253*(1), 47-54.
- Fernandez-Trillo, F., Grover, L. M., Stephenson-Brown, A., Harrison, P., & Mendes, P. M. (2017). Vesicles in nature and the laboratory: elucidation of their biological properties and synthesis of increasingly complex synthetic vesicles. *Angewandte Chemie International Edition*, *56*(12), 3142-3160.

- Field, C. J. (2005). The immunological components of human milk and their effect on immune development in infants. *The Journal of nutrition*, *135*(1), 1-4.
- Fujita, K., Tanaka, S., Iizumi, K., Akiyama, S., Uchida, K., Ogata, M., ... & Kubohara, Y. (2019). Melibiosamine, a novel oligosaccharide, suppresses mitogen-induced IL-2 production via inactivation of NFAT and NFκB in Jurkat cells. *Biochemistry and biophysics reports*, *19*, 100658.
- Gasser, A., Glassmeier, G., Fliegert, R., Langhorst, M. F., Meinke, S., Hein, D., ... & Guse, A. H. (2006). Activation of T cell calcium influx by the second messenger ADP-ribose. *Journal of Biological Chemistry*, *281*(5), 2489-2496.
- Gauttier, V., Pengam, S., Durand, J., Biteau, K., Mary, C., Morello, A., ... & Poirier, N. (2020). Selective SIRPα blockade reverses tumor T cell exclusion and overcomes cancer immunotherapy resistance. *The Journal of clinical investigation*, *130*(11), 6109-6123.
- Gdalevich, M., Mimouni, D., David, M., & Mimouni, M. (2001). Breast-feeding and the onset of atopic dermatitis in childhood: a systematic review and meta-analysis of prospective studies. *Journal of the American Academy of Dermatology*, *45*(4), 520-527.
- Gillespie, M., Jassal, B., Stephan, R., Milacic, M., Rothfels, K., Senff-Ribeiro, A., ... & D'Eustachio, P. (2022). The reactome pathway knowledgebase 2022. *Nucleic acids research*, *50*(D1), D687-D692.
- Gómez-Angelats, M., Bortner, C. D., & Cidlowski, J. A. (2000). Protein kinase C (PKC) inhibits fas receptor-induced apoptosis through modulation of the loss of K+ and cell shrinkage: a role for PKC upstream of caspases. *Journal of Biological Chemistry*, *275*(26), 19609-19619.
- Gopalakrishna, K. P., Macadangdang, B. R., Rogers, M. B., Tometich, J. T., Firek, B. A., Baker, R., ... & Hand, T. W. (2019). Maternal IgA protects against the development of necrotizing enterocolitis in preterm infants. *Nature medicine*, *25*(7), 1110-1115.
- Harding, F. A., Mcarthur, J. G., Gross, J. A., Raulet, D. H., & Allison, J. P. (1992). CD28-mediated signalling co-stimulates murine T cells and prevents induction of anergy in T-cell clones. *Nature*, 607–609.
- Ilboudo, A., Nault, J. C., Dubois-Pot-Schneider, H., Corlu, A., Zucman-Rossi, J., Samson, M., & Le Seyec, J. (2014). Overexpression of phosphatidylinositol 4-kinase type IIIα is

associated with undifferentiated status and poor prognosis of human hepatocellular carcinoma. *BMC cancer*, *14*(1), 1-8.

- Jacobs, S. R., Herman, C. E., MacIver, N. J., Wofford, J. A., Wieman, H. L., Hammen, J. J., & Rathmell, J. C. (2008). Glucose uptake is limiting in T cell activation and requires CD28-mediated Akt-dependent and independent pathways. *The Journal of Immunology*, *180*(7), 4476-4486.
- Jaffar, Z. H., Stanciu, L., Pandit, A., Lordan, J., Holgate, S. T., & Roberts, K. (1999). Essential role for both CD80 and CD86 costimulation, but not CD40 interactions, in allergen-induced Th2 cytokine production from asthmatic bronchial tissue: Role for αβ, but not γδ, T cells. *The Journal of Immunology*, *163*(11), 6283-6291.
- Jutz, S., Leitner, J., Schmetterer, K., Doel-Perez, I., Majdic, O., Grabmeier-Pfistershammer, K., ... & Steinberger, P. (2016). Assessment of costimulation and coinhibition in a triple parameter T cell reporter line: Simultaneous measurement of NF-κB, NFAT and AP-1. *Journal of immunological methods*, *430*, 10-20.
- Klíma, M., Broučková, A., Koc, M., & Anděra, L. (2011). T-cell activation triggers death receptor-6 expression in a NF-κB and NF-AT dependent manner. *Molecular Immunology*, *48*(12-13), 1439-1447.
- Korkut, C., Ataman, B., Ramachandran, P., Ashley, J., Barria, R., Gherbesi, N., & Budnik, V. (2009). Trans-synaptic transmission of vesicular Wnt signals through Evi/Wntless. *Cell*, *139*(2), 393-404.
- Larché, M., Till, S. J., Haselden, B. M., North, J., Barkans, J., Corrigan, C. J., ... & Robinson, D. S. (1998). Costimulation through CD86 is involved in airway antigen-presenting cell and T cell responses to allergen in atopic asthmatics. *The Journal of Immunology*, *161*(11), 6375-6382.
- Lässer, C., Seyed Alikhani, V., Ekström, K., Eldh, M., Torregrosa Paredes, P., Bossios, A., ... & Valadi, H. (2011). Human saliva, plasma and breast milk exosomes contain RNA: uptake by macrophages. *Journal of translational medicine*, *9*(1), 1-8.
- Macian, F. (2005). NFAT proteins: key regulators of T-cell development and function. *Nature Reviews Immunology*, *5*(6), 472-484.
- Meuer, S. C., Fitzgerald, K. A., Hussey, R. E., Hodgdon, J. C., Schlossman, S. F., & Reinherz, E. L. (1983). Clonotypic structures involved in antigen-specific human T cell

function. Relationship to the T3 molecular complex. *The Journal of experimental medicine*, *157*(2), 705-719.

- Mowat, A. M. (2018). To respond or not to respond—a personal perspective of intestinal tolerance. *Nature Reviews Immunology*, *18*(6), 405-415.
- Palmeira, P., Quinello, C., Silveira-Lessa, A. L., Zago, C. A., & Carneiro-Sampaio, M. (2012). IgG placental transfer in healthy and pathological pregnancies. *Clinical and Developmental Immunology*, *2012*.
- Pereira, P. C. (2014) Milk nutritional composition and its role in human health. *Nutrition* 30, 619–627
- Rincon, M., & Flavell, R. A. (1994). AP-1 transcriptional activity requires both T-cell receptor-mediated and co-stimulatory signals in primary T lymphocytes. *The EMBO journal*, *13*(18), 4370-4381.
- Rosskopf, S., Leitner, J., Paster, W., Morton, L. T., Hagedoorn, R. S., Steinberger, P., & Heemskerk, M. H. (2018). A Jurkat 76 based triple parameter reporter system to evaluate TCR functions and adoptive T cell strategies. *Oncotarget*, *9*(25), 17608.
- Schmiedel, B. J., Singh, D., Madrigal, A., Valdovino-Gonzalez, A. G., White, B. M., Zapardiel-Gonzalo, J., ... & Vijayanand, P. (2019). Impact of genetic polymorphisms on human immune cell gene expression. (https://dice-database.org/landing)
- Semmes, E. C., Chen, J. L., Goswami, R., Burt, T. D., Permar, S. R., & Fouda, G. G. (2021). Understanding early-life adaptive immunity to guide interventions for pediatric health. *Frontiers in Immunology*, *11*, 595297.
- Siska, P. J., van der Windt, G. J., Kishton, R. J., Cohen, S., Eisner, W., MacIver, N. J., ... & Rathmell, J. C. (2016). Suppression of Glut1 and glucose metabolism by decreased Akt/mTORC1 signaling drives T cell impairment in B cell leukemia. *The Journal of Immunology*, *197*(6), 2532-2540.
- Smart, J. M., & Kemp, A. S. (2002). Increased Th1 and Th2 allergen-induced cytokine responses in children with atopic disease. *Clinical & Experimental Allergy*, *32*(5), 796-802.
- Takimoto, C. H., Chao, M. P., Gibbs, C., McCamish, M. A., Liu, J., Chen, J. Y., ... & Weissman, I. L. (2019). The Macrophage 'Do not eat me'signal, CD47, is a clinically validated cancer immunotherapy target. *Annals of Oncology*, *30*(3), 486-489.

- Tkach, M., Kowal, J., & Théry, C. (2018). Why the need and how to approach the functional diversity of extracellular vesicles. *Philosophical Transactions of the Royal Society B: Biological Sciences*, *373*(1737), 20160479.
- Turner, D. L., & Farber, D. L. (2014). Mucosal resident memory CD4 T cells in protection and immunopathology. *Frontiers in immunology*, *5*, 331.
- van Herwijnen, M. J., Zonneveld, M. I., Goerdayal, S., Nolte, E. N., Garssen, J., Stahl, B., ... & Wauben, M. H. (2016). Comprehensive proteomic analysis of human milk-derived extracellular vesicles unveils a novel functional proteome distinct from other milk components. *Molecular & Cellular Proteomics*, *15*(11), 3412-3423.
- van Leeuwen, J. E., & Samelson, L. E. (1999). T cell antigen-receptor signal transduction. *Current opinion in immunology*, *11*(3), 242-248.
- Varcianna, A., Myszczynska, M. A., Castelli, L. M., O'Neill, B., Kim, Y., Talbot, J., ... & Ferraiuolo, L. (2019). Micro-RNAs secreted through astrocyte-derived extracellular vesicles cause neuronal network degeneration in C9orf72 ALS. *EBioMedicine*, *40*, 626-635.
- Wambre, E., James, E. A., & Kwok, W. W. (2012). Characterization of CD4+ T cell subsets in allergy. *Current opinion in immunology*, *24*(6), 700-706.
- Zhang, Z., Tang, Z., Ma, X., Sun, K., Fan, L., Fang, J., ... & Zhou, J. (2018). TAOK1 negatively regulates IL-17-mediated signaling and inflammation. *Cellular & molecular immunology*, *15*(8), 794-802.
- Zhao, Y., Altman, B. J., Coloff, J. L., Herman, C. E., Jacobs, S. R., Wieman, H. L., ... & Rathmell, J. C. (2007). Glycogen synthase kinase 3α and 3β mediate a glucose-sensitive antiapoptotic signaling pathway to stabilize Mcl-1. *Molecular and cellular biology*, *27*(12), 4328-4339.
- Zhou, Q., Li, M., Wang, X., Li, Q., Wang, T., Zhu, Q., ... & Li, X. (2012). Immune-related microRNAs are abundant in breast milk exosomes. *International journal of biological sciences*, *8*(1), 118.
- Zitvogel, L., Regnault, A., Lozier, A., Wolfers, J., Flament, C., Tenza, D., ... & Amigorena, S. (1998). Eradication of established murine tumors using a novel cell-free vaccine: dendritic cell derived exosomes. *Nature medicine*, *4*(5), 594-600.

- Zonneveld, M.I., van Herwijnen, M.J., Fernandez-Gutierrez, M.M., Giovanazzi, A., de Groot, A.M., Kleinjan, M., van Capel, T.M., Sijts, A.J., Taams, L.S., Garssen, J. and de Jong, E.C., 2021. Human milk extracellular vesicles target nodes in interconnected signalling pathways that enhance oral epithelial barrier function and dampen immune responses. *Journal of extracellular vesicles*, *10*(5), p.e12071.

Supplementary documents

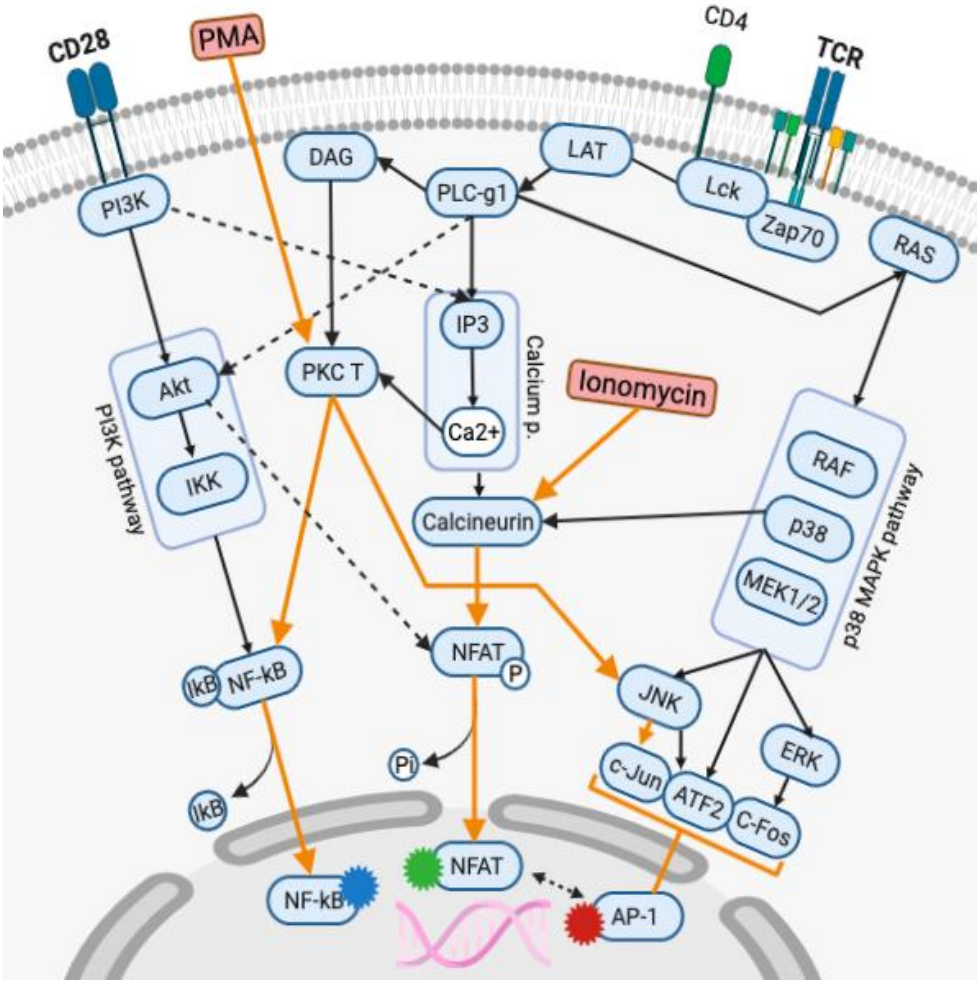

Fig. S1: Summary scheme representing engaged pathways of T cell activation in response to PMA/Ionomycin stimulation.

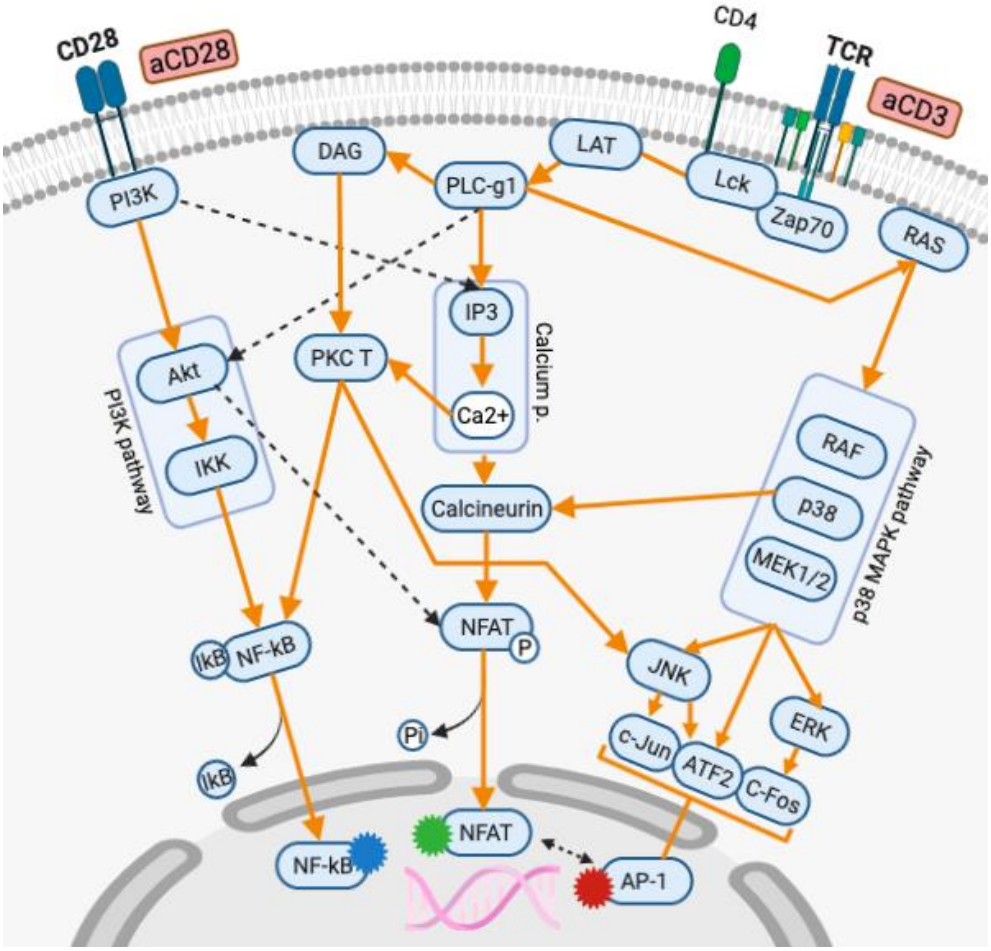

Fig. S2: Summary scheme representing engaged pathways of T cell activation in response to anti-CD3/anti-CD28 stimulation.

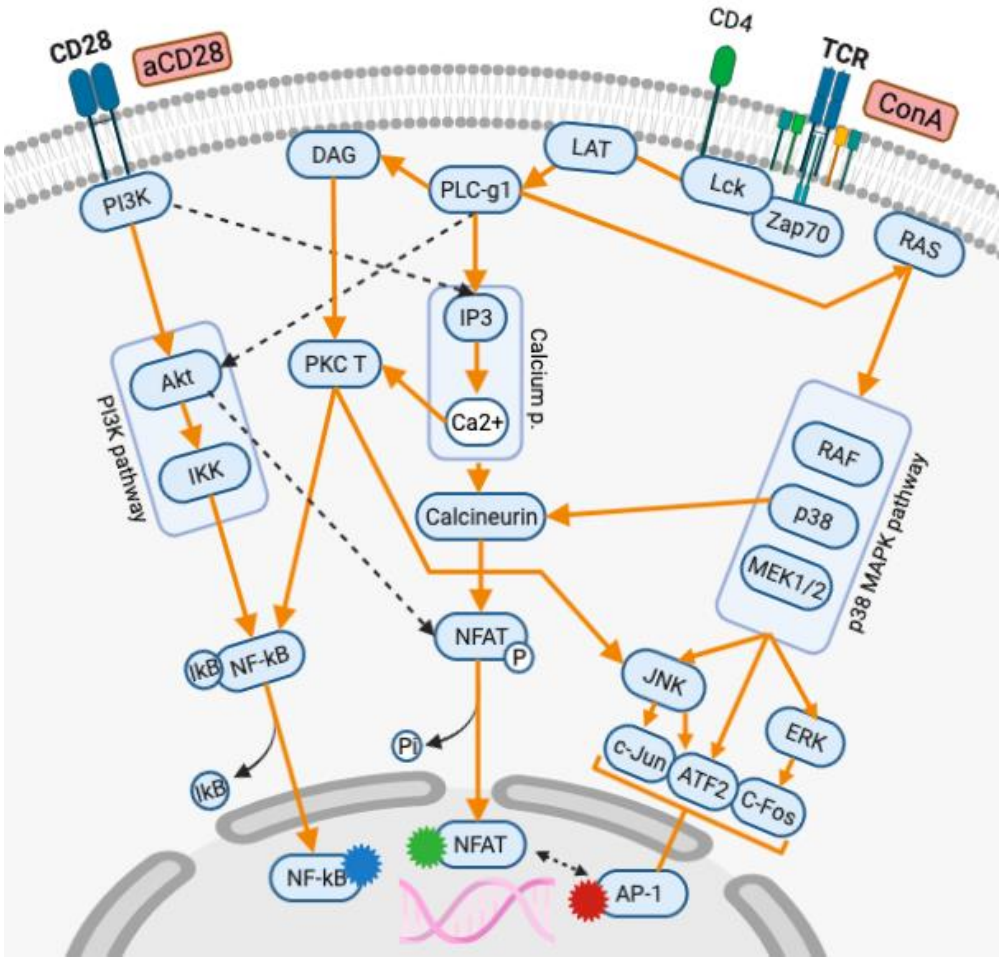

Fig. S3: Summary scheme representing engaged pathways of T cell activation in response to Concanavalin A and anti-CD28 stimulation.

Type	Donor	Age (y)	Parity	Weeks after delivery	Total IgE (kU/mL)	ImmunoCAP Phadiatop ratio	Specific IgE against allergen
Non-allergic	D10	34	4	5	24.7	0.2	All below detection limit
	D17	31	2	5	27.8	0.2	All below detection limit
	D18	35	2	13	15.8	0.2	All below detection limit
	D30	36	1	8	38.9	0.2	All below detection limit
	D36	31	1	5	30.4	0.1	All below detection limit
	D40	33	3	6	9.6	0.2	All below detection limit
Allergic	D8	30	2	9	73.6	13.8	Grass pollen <0.35; tree pollen 7.6; house dust mite 1.0; cat dander <0.35; dog dander <0.35
	D14	34	2	6	243	53.6	Grass pollen <0.97; tree pollen 40; house dust mite 4.2; cat dander <0.35; dog dander <0.35
	D19	37	4	5	87.5	45.2	Grass pollen 32; tree pollen 5.0; house dust mite 6.4; cat dander <0.35; dog dander <0.35
	D25	32	2	6	141	6.6	Grass pollen <0.35; tree pollen <0.35; house dust mite 3.8; cat dander <0.35; dog dander <0.35
	D29	29	1	8	226	58.6	Grass pollen 0.36; tree pollen 0.35; house dust mite 41 ; cat dander 1.1; dog dander 0.64
	D31	25	1	7	81.9	27.4	Grass pollen 1.3; tree pollen 7.7; house dust mite 4.4; cat dander 0.49; dog dander 1.1

Fig. S4: Table summary of data from donors of the ACCESS study. Informaiton provided include Donor name, age, parity, weeks after birth at time of donation, IgE titers (kU/mL), ImmunoCAP Phadiatop assay ratio results, allergen-specific IgE in parental serum. These details were used to classify the donors as allergic or non-allergic.

Fraction	Iodixanol (%)	Volume 50% optiprep (ml)	Volume 1x PBS(ml)
1	50.0	2.000	0
2	47.1	1.884	0.116
3	44.3	1.772	0.228
4	41.4	1.656	0.344
5	38.6	1.544	0.456
6	35.7	1.428	0.572
7	32.9	1.316	0.684
8	30.0	1.200	0.800
9	27.1	1.084	0.916
10	24.3	0.972	1.028
11	21.4	0.856	1.144
12	18.6	0.744	1.256
13	15.7	0.628	1.372
14	12.9	0.516	1.484
15	10.0	0.400	1.600

Fig. S5: Table detailing the compositions of the Optiprep fractions used in the EV isolation procedure.

Parameter	Gain
FSC	82
SSC	101
525-40 (488)	82
610-20 (488)	125
690-50 (488)	272
585-42 (561)	280
610-20 (561)	261
675-30 (561)	251
710-50 (561)	227
763-43 (561)	1256
450-45 (405)	59
525-40 (405)	33
610-20 (405)	188
660-10 (405)	169
763-43 (405)	354

Fig. S6: Table representing acquisition gains consistent throughout all flow cytometry measurements.

	Unstimulated		Stimulated	
	replicates	average	replicates	average
NFAT	1460		23299	
	1426		22073	
	1476	1454	20755	22042
NF-kB	1056		43809	
	1024		41168	
	1083	1054	38586	41188
AP-1	804		1270	
	780		1259	
	810	798	1266	1256

Fig. S7: Table collecting geoMFI data used in the bar graph comparing reporter signals in unstimulated and PMA/Ionomycin stimulated TPR cells (Figure 3B). This table includes the three technical replicates performed, which were averaged to obtain values used in the bar graph.

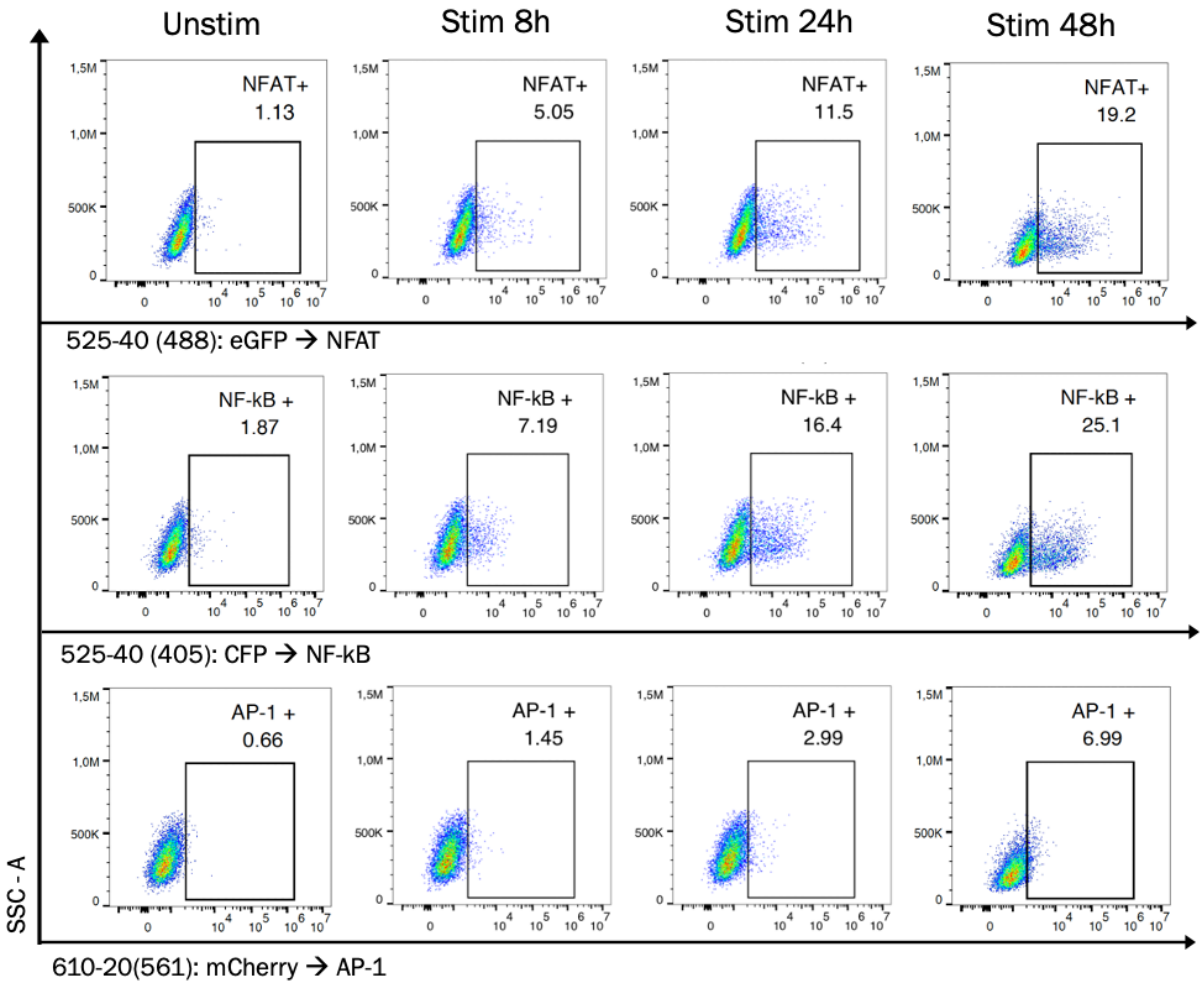

Fig. S8: Representative dot plots of positively gated TPR cells for all three reporters (NFAT-eGFP, NF-kB - CFP, AP-1 – mCherry) in the following conditions: Unstimulated, Stimulated with anti-CD3 and 2.5 ug/mL anti-Cd28 for 8 hours, stimulated for 24 hours and stimulated for 48 hours. Samples were performed in triplicates (n=3) which are not shown here.

	Unstimulated		Stimulated 8h		Stimulated 24h		Stimulated 48h	
	replicates	average	replicates	average	replicates	average	replicates	average
NFAT	1253		1448		1784		1794	
	1249		1404		1843		2270	
	1270	1257	1272	1375	1907	1845	2329	2131
NF-kB	1952		2138		2820		3019	
	1905		2132		2433		2959	
	1934	1930	2017	2095	2483	2579	2563	2847
AP-1	696		739		955		1047	
	680		738		807		1028	
	692	689	718	732	840	867	1053	1042

Fig. S9: Table collecting geoMFI data used in the bar graph comparing reporter signals in unstimulated and aCD3/aCD28 stimulated TPR cells (Figure). Each condition includes three technical replicates, and their average values were also included.

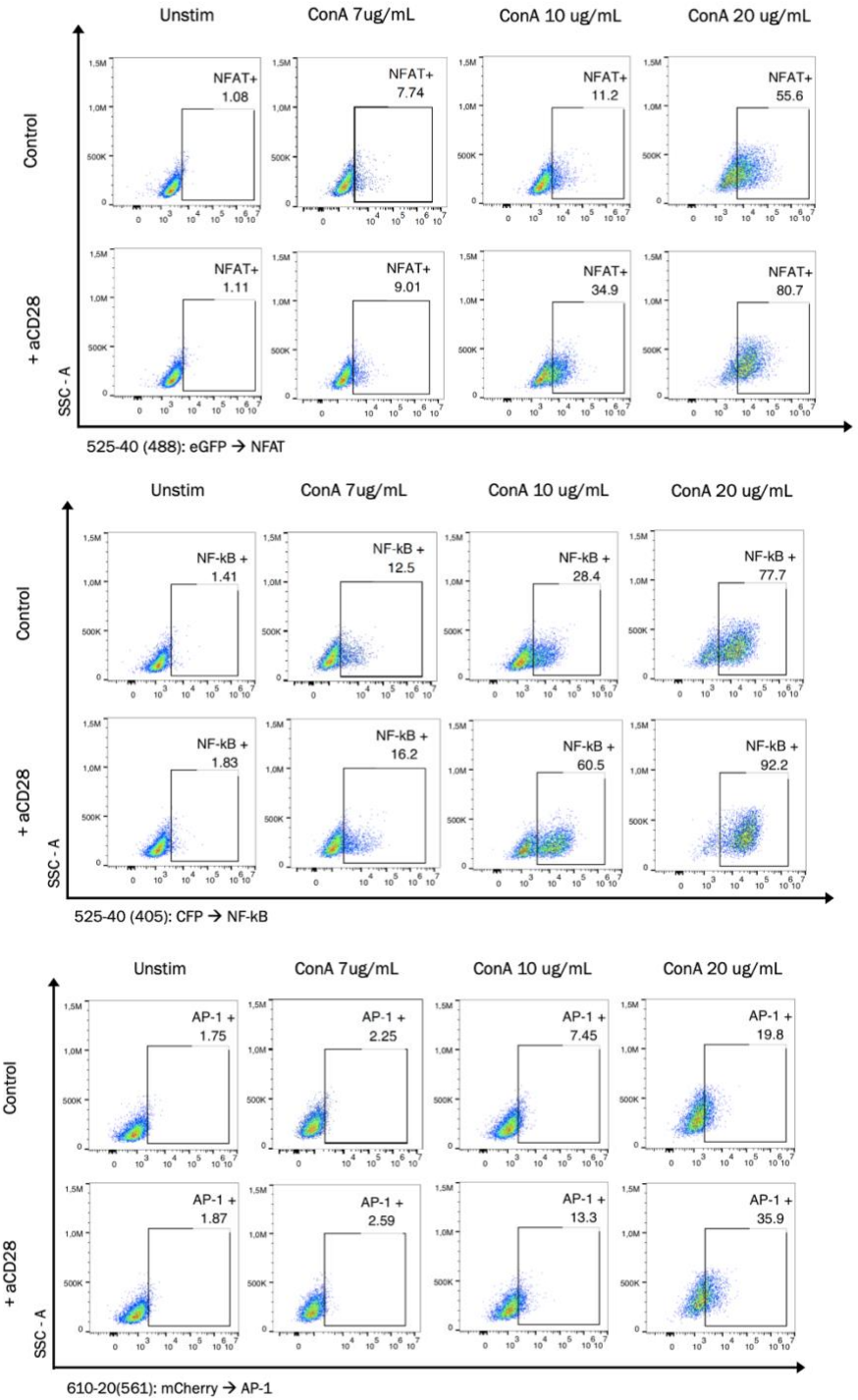

Fig. S10: Representative dot plots of the positively gated TPR cells for each reporter signal (NFAT – eGFP, NF-kB – CFP, AP-1 – mCherry) in unstimulated, 7ug/mL of ConA, 10ug/mL of ConA, 20 ug/mL of ConA, and all these conditions with an added 2.5 ug/mL of aCD28.
The 7ug/mL of ConA was obtained from a different experiment compared to the other conditons but parameters were maintained identical.

NFAT	ConA only (triplicate MFI average)	ConA + 2.5 ug/mL aCD28 (tripl. MFI average)	Percentage increase (in %)
5 ug/mL (v.1)	1624	1663	2
7 ug/mL	1813	1833	1
10 ug/mL (v.1)	2998	4328	44
10 ug/mL (v.2)	2605	4533	74
10 ug/mL (v.3)	2312	3880	67
10 ug/mL (v.4)	2891	4551	57
20 ug/mL (v.1)	7406	12087	63
20 ug/mL (v.2)	7319	11460	57
40 ug/mL	10493	13419	27

NF-kB	ConA only (triplicate MFI average)	ConA + 2.5 ug/mL aCD28 (tripl. MFI average)	Percentage increase (in %)
5 ug/mL (v.1)	1157	1278	10
7 ug/mL	1422	1576	11
10 ug/mL (v.1)	2455	6071	147
10 ug/mL (v.2)	2132	6697	214
10 ug/mL (v.3)	2091	6052	189
10 ug/mL (v.4)	2230	5954	167
20 ug/mL (v.1)	9702	23442	142
20 ug/mL (v.2)	9420	19840	111
40 ug/mL	11293	18183	61

AP-1	ConA only (triplicate MFI average)	ConA + 2.5 ug/mL aCD28 (tripl. MFI average)	Percentage increase (in %)
5 ug/mL (v.1)	900	904	0.5
7 ug/mL	959	934	-3
10 ug/mL (v.1)	1154	1274	10
10 ug/mL (v.2)	1137	1320	16
10 ug/mL (v.3)	1074	1183	10
10 ug/mL (v.4)	1128	1248	11
20 ug/mL (v.1)	1473	1900	29
20 ug/mL (v.2)	1425	1778	25
40 ug/mL	1337	1608	20

Fig. S11: Tables representing collected geoMFI data used in the bar graph of the added value of aCD28 at different conA concentrations. Each data point is an averaged value of technical replicates (n=3). The conditions were experimentally repeated as follows: 5 ug/mL (n=1), 7 ug/mL (n=1), 10 ug/mL (n=4), 20 ug/mL (n= 2) and 40 ug/mL (n=1). Each table contains data for one reporter signal.

NFAT table	Experiment 1	Experiment 2	Experiment 3
Unstimulated	1454	1933	1933
ConA	2312	2891	N/A
ConA + EV	1857	1926	N/A
ConA + EVd	2111	2461	N/A
ConA/aCD28	4533	3879	4551
ConA/aCD28 + EV	1966	2016	2163
ConA/aCD28 + EVd	3011	2642	2804

Fig. S12: Table of the averaged geometric mean fluorescence intensities (geoMFIs) used in the bar graph representing NFAT reporter (eGFP) signal in different conditions: unstimulated; TPR cells stimulated by 10ug/mL of ConA only and exposed to EVs and EV depleted samples; TPR cells stimulated with 10ug/mL of ConA + 2.5 ug/mL of aCD28 and exposed to the same EV and EV depleted samples**.** Each value is an average of technical triplicates values (unstimulated, ConA control, ConA + aCD28 control) or biological triplicates (EV and EV depleted samples from three donors. **The** EV/EVd effect on ConA experiment as repeated once whereas the EV/EVd effect on ConA+aCD28 was repeated twice.

NF-kB table	Experiment 1	Experiment 2	Experiment 3
Unstimulated	1054	1176	1152
ConA	2091	2230	N/A
ConA + EV	1180	1215	N/A
ConA + EVd	1454	1722	N/A
ConA/aCD28	6697	6052	5954
ConA/aCD28 + EV	1574	1529	1616
ConA/aCD28 + EVd	3321	2692	2441

Fig. S13: Table of the averaged geometric mean fluorescence intensities (geoMFIs) used in the bar graph representing NF-kB reporter (CFP) signal in different conditions: unstimulated; TPR cells stimulated by 10ug/mL of ConA only and exposed to EVs and EV depleted samples; TPR cells stimulated with 10ug/mL of ConA + 2.5 ug/mL of aCD28 and exposed to the same EV and EV depleted samples**.** Each value is an average of technical triplicates values (unstimulated, ConA control, ConA + aCD28 control) or biological triplicates (EV and EV depleted samples from three donors. **The** EV/EVd effect on ConA experiment as repeated once whereas the EV/EVd effect on ConA+aCD28 was repeated twice.

AP-1 table	Experiment 1	Experiment 2	Experiment 3
Unstimulated	798	858	956
ConA	1074	1127	N/A
ConA + EV	915	874	N/A
ConA + EVd	965	1031	N/A
ConA/aCD28	1320	1183	1247
ConA/aCD28 + EV	889	932	894
ConA/aCD28 + EVd	1073	1004	1004

Fig. S14: Table of the averaged geometric mean fluorescence intensities (geoMFIs) used in the bar graph representing AP-1 reporter (mCherry) signal in different conditions: unstimulated; TPR cells stimulated by 10ug/mL of ConA only and exposed to EVs and EV depleted samples; TPR cells stimulated with 10ug/mL of ConA + 2.5 ug/mL of aCD28 and exposed to the same EV and EV depleted samples. Each value is an average of technical triplicates values (unstimulated, ConA control, ConA + aCD28 control) or biological triplicates (EV and EV depleted samples from three donors. The EV/EVd effect on ConA experiment as repeated once whereas the EV/EVd effect on ConA+aCD28 was repeated twice.

	Unstimulated		Stimulated		Stim + Allergic EVs		Stim + Non-allergic EVs	
	Technical replicates	Average	Technical replicates	Average	Biological Replicates	Average	Biological Replicates	Average
NFAT	1388	1410	3619	3702	2890	3047	2141	2231
					2983		2132	
	1412		3841		2582		2188	
					3156		2497	
	1430		3646		3242		2076	
					3430		2350	
NF-kB	1047	1054	5971	6063	4257	4665	1791	1998
					4734		1730	
	1054		6465		3576		2008	
					4884		2578	
	1060		5753		5059		1638	
					5480		2243	
AP-1	1023	1031	1493	1506	1260	1290	1120	1150
					1263		1132	
	1043		1524		1191		1114	
					1302		1220	
	1026		1502		1341		1139	
					1381		1173	

Fig. S15: Table collecting the individual and averaged geometric Mean Fluorescence Intensities (geoMFI) measurements for NFAT (eGFP), NF-kB (CFP) and AP-1 (mCherry) signals from TPR cells in different conditions: Unstimulated, stimulated with 10ug/mL of ConA and 2.5 ug/mL of aCD28, stimulated in presence of EVs derived from allergic donors, stimulated in presence of EVs from healthy donors. The unstimulated and stimulated controls were performed in technical triplicates whereas 6 biological replicates (EV donors) were used for Allergic and non-allergic groups.

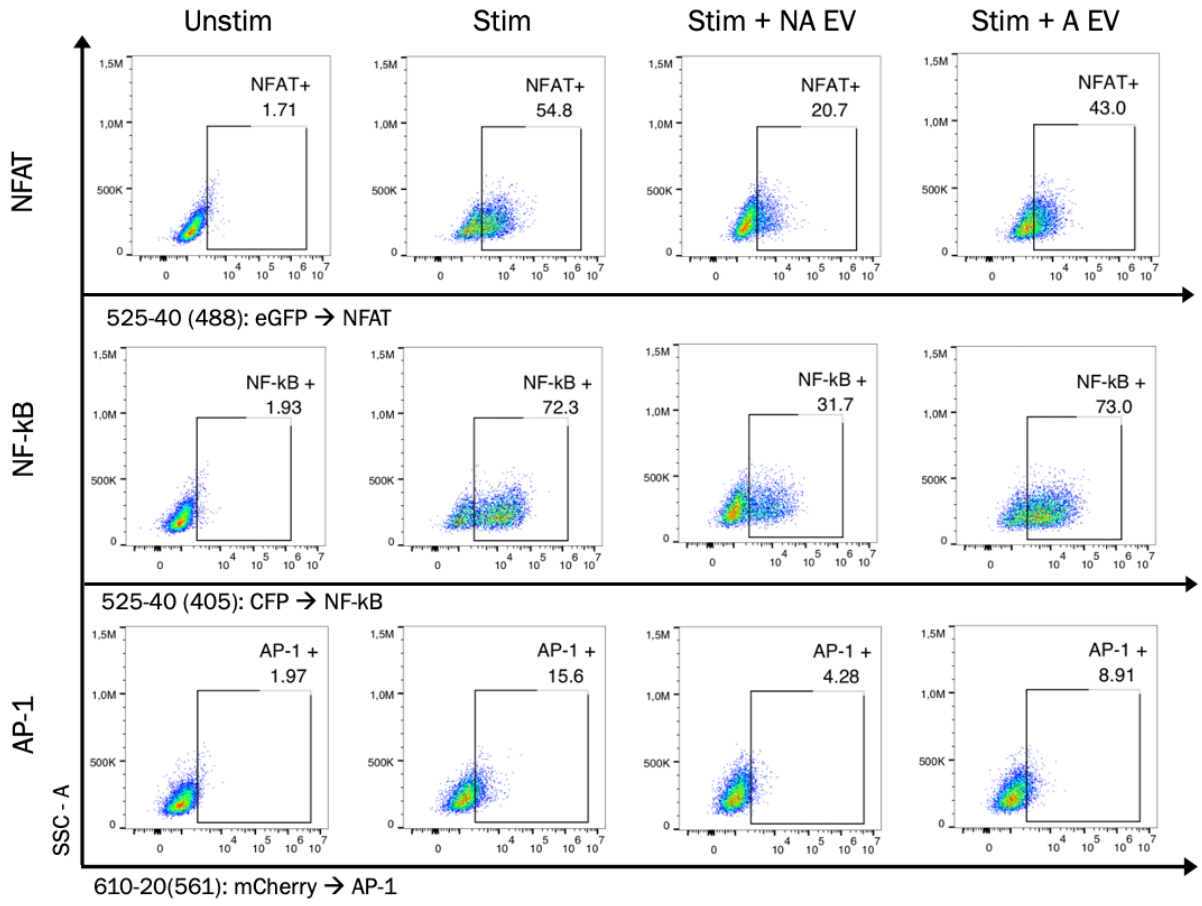

Fig. S16: Representative dot plots of positively gated TPR cells for all three reporter signals: NFAT (eGFP), NF-kB (CFP), AP-1 (mCherry) in different conditions: Unstimulated, stimulated with 10ug/mL of ConA and 2.5 ug/mL of aCD28, stimulated in presence of EVs derived from allergic donors, stimulated in presence of EVs from healthy donors
The technical replicates for controls (n=3) and biological replicates for EV samples (n=6) were not shown.